




EX LIBRIS
UNIVERSITATIS
ALBERTENSIS

The Bruce Peel
Special Collections
Library



Digitized by the Internet Archive
in 2025 with funding from
University of Alberta Library

<https://archive.org/details/0162014234122>

University of Alberta

Library Release From

Name of Author: Chun Lu

Title of Thesis: A Field Study on Oxygen Penetration into Wastewater Biofilms

Degree: Master of Science

Year this Degree Granted: 2001

Permission is hereby granted to the University of Alberta Library to reproduce single copies of this thesis and to lend or sell such copies for private, scholarly or scientific research purposes only.

The author reserves all other publication and other rights in association with the copyright in the thesis, and except as herein before provided, neither the thesis nor any substantial portion thereof may be printed or otherwise reproduced in any material form whatever without the author's prior written permission.

University of Alberta

A Field Study On Oxygen Penetration Into Wastewater Biofilms

By

Chun Lu



A thesis submitted to the Faculty of Graduate Studies and Research in partial fulfillment of the requirements for the degree of Master of Science

In

Environmental Science

Department of Civil and Environmental Engineering

Edmonton, Alberta

Fall 2001

University of Alberta

Faculty of Graduate Studies and Research

The undersigned certify that they have read, and recommend to the Faculty of Graduate Studies and Research for acceptance, a thesis entitled *A Field Study On Oxygen Penetration Into Wastewater Biofilms* submitted By *Chun Lu* in partial fulfillment of the requirements for the degree of *Master of Science in Environmental Science*.

ABSTRACT

This thesis includes two parts. The first part contains the theory, fabrication and evaluation of a combined oxygen microelectrode. This oxygen microelectrode is not easily subject to external electromagnetic interference, hence suitable for *in-situ* measurement in biofilms under field conditions.

The second part is a field study on oxygen penetration into wastewater biofilms in two typical municipal wastewater treatment plants using the oxygen microelectrode. Twenty-four dissolved oxygen profiles along the depth of biofilms at different stages of the rotating biological contactors were measured.

The results of this study confirmed that oxygen depletion is a common phenomenon in wastewater biofilms under field conditions. In all measurements, the oxygen penetration depth was less than 0.6 mm. No full oxygen penetration in biofilms was observed. The results also disclosed that the oxygen penetration depth in biofilms with shorter length of operation is greater than that in biofilms with longer length of operation.

Acknowledgements

My profound gratitude goes to my academic supervisor, Dr. Tong Yu, without whom this thesis would not be possible. I thank him for his research advising, thesis reviewing as well as stable financial supporting throughout this thesis study.

I would like to express my appreciation to Nick Chernuka, Gary Solonyanko, Debra Long, and Walter Moranetz. Their helps in providing laboratory facilities made this research go very smoothly.

My special thanks go to Andy Bebbington, Jim Hepler and Dave Barabash at the Water and Wastewater Treatment Plant, Town of Devon and Tom Graham at the Wastewater Treatment Plant, Town of Olds. Without their cooperation, the field work of this thesis would be impossible.

My special thanks also extend to my co-workers in Dr. Yu's research group, Carlos de la Rosa and Omar Lopez, for their working with me and providing great help in biofilm measurements under harsh field conditions.

I would also like to thank members of the thesis examining committee, Dr. Mike Belosevic, Dr. Ian Buchanan, Dr. Xiaoqi (Jackie) Zhang, for their insights and suggestions on the revision of this thesis.

Finally, I want to express my thanks to my wife, Lan, and our parents far away from us, for their love and support.

TABLE OF CONTENTS

Chapter 1 Introduction.....	1
Chapter 2 Fabrication and Evaluation of Oxygen Microelectrode	5
2.1 Theory of oxygen microelectrode	5
2.2 Development of oxygen microelectrode	8
2.2.1 The separate oxygen microelectrode.....	9
2.2.2 The combined oxygen microelectrode	12
2.2.3 Comparisons of oxygen microelectrodes	17
2.3 Fabrication of oxygen microelectrode	18
2.4 Evaluation of oxygen microelectrode	27
2.4.1 Polarization and calibration methods	27
2.4.2 Calibration results and discussions	30
Chapter 3 Field Study on Oxygen Penetration in Wastewater Biofilms.....	37
3.1 Introduction.....	37
3.2 Site selection for field study.....	42
3.3 Materials and methods	46
3.4 Results and discussions.....	52
3.4.1 Determination of biofilm surface	52
3.4.2 DO profiles in wastewater biofilms	56
3.4.3 Oxygen penetration depth in wastewater biofilms.....	61
3.4.4 Comparison of DO penetration depth between different RBC stages ...	64
3.4.5 Comparison of DO penetration depth between different substrata	66
3.4.6 Comparison of DO penetration depth between different plants.....	68
3.4.7 Estimation of oxygen flux into wastewater biofilms	71
Chapter 4 Conclusions and Recommendations.....	76

4.1 Conclusions.....	76
4.2 Recommendations for future work	78
References	80
Appendices	87

LIST OF TABLES

Table 2.1	Comparisons of oxygen microelectrodes.....	18
Table 2.2	Results of oxygen unit conversion and data for Figure 2.6.....	33
Table 3.1	Major characteristics of RBC systems at Devon and Olds.....	44
Table 3.2	Water quality in RBC systems at Devon and Olds.....	45
Table 3.3	DO penetration depths in biofilms at Devon and Olds.....	62
Table 3.4	Comparison of DO penetration depth between different RBC stages.....	64
Table 3.5	Comparison of DO penetration depth between different substrata.....	67
Table 3.6	Comparison of DO penetration depth between different plants.....	69
Table 3.7	DO penetration depths and the start-up time of RBC stages.....	70
Table 3.8	Oxygen flux into biofilms at each RBC stage at Devon and Olds.....	74

LIST OF FIGURES

Figure 2.1	Current-voltage curve.....	7
Figure 2.2	Schematic diagram of a combined oxygen microelectrode with a guard Cathode.....	19
Figure 2.3	Schematic diagram for tapering of the working cathode tip.....	22
Figure 2.4	Calibration for an oxygen microelectrode.....	30
Figure 2.5	Calibration curve for an oxygen microelectrode (current signal vs oxygen volume fraction in dry calibration gas).....	32
Figure 2.6	Calibration curve for an oxygen microelectrode (current signal vs dissolved oxygen concentration).....	34
Figure 3.1	Schematic diagram of the RBC system.....	43
Figure 3.2	Setup for DO measurement in RBC biofilms using an oxygen Microelectrode.....	47
Figure 3.3	Thickness of attached water film on RBC disc as a function of $\omega^{1/2}$	54
Figure 3.4	Determination of the biofilm surface.....	55
Figure 3.5	DO profiles in biofilms at Stage 1 at Olds.....	75
Figure 3.6	DO profiles in biofilms at Stage 2 at Olds	57
Figure 3.7	DO profiles in biofilms at Stage 3 at Olds.....	58
Figure 3.8	DO profiles in biofilms at Stage 4 at Olds.....	58
Figure 3.9	DO profiles in biofilms at Stage 1 at Devon.....	59
Figure 3.10	DO profiles in biofilms at Stage 2 at Devon.....	59
Figure 3.11	DO profiles in biofilms at Stage 3 at Devon.....	60

Figure 3.12 DO profiles in biofilms at Stage 4 at Devon.....	60
Figure 4.13 Comparison of DO penetration depth between different RBC stages.....	66
Figure 4.14 Comparison of DO penetration depth between different substrata.....	68

Chapter 1 Introduction

In biological wastewater treatment processes, there are generally two groups of bioreactors. One is the suspended growth bioreactor. The other is the attached growth bioreactor. In comparison with the suspended growth bioreactor, the attached growth bioreactor has some advantages such as the ability to support a variety of microbial populations at various locations within the biofilm that may degrade different organic substrates. Therefore, the latter type of bioreactor has been employed widely in environmental engineering. As its name implies, one main reason for the success of the attached growth bioreactor in wastewater treatment is the existence of the unique biofilm growing on a solid surface of the bioreactor.

In order for the wastewater biofilm to be functional in wastewater treatment, the electron donors, the electron acceptors and other nutrients must be transferred into the biofilm and reaction products from the biofilm into the wastewater. As a result, apart from biochemical reactions occurring in the biofilm, mass transfer in the biofilm is one of the important considerations in understanding the nature of biofilms.

Oxygen acts as an electron acceptor in biochemical reactions such as carbon oxidization and nitrification occurring in wastewater biofilms. The level of dissolved oxygen (DO) plays a key role in the development of various microorganism communities, which in turn play different roles in substrate removals in wastewater treatment. As a result, availability of oxygen in wastewater biofilms, technically, is an important parameter in bioreactor designing and operation. Economically, oxygen

requirement has great impact on the operating costs of the wastewater treatment system. A good understanding on oxygen penetration and oxygen flux into wastewater biofilms is essential for the rational optimization of biofilm reactor design and operation.

A number of laboratory work has already been done on DO transfer in biofilms (Whalen *et al.*, 1969; Chen and Bungay, 1981; Kuenen *et al.*, 1986; Nishidome *et al.*, 1988 and 1994; Fu, 1993; Zhang, 1994; Yu, 2000), but research results directly obtained from wastewater biofilm systems in the field are rare. One major reason is the lack of suitable study tools for *in-situ* DO observation in wastewater biofilms under field conditions.

Biofilms comprise clusters of microorganisms and voids. They are very complex environments resistant to many of the traditional analytical techniques used in microbial ecology (Ward *et al.*, 1992). Therefore, tools with high spatial resolutions on micro-scale are very crucial to biofilm study. Microelectrodes, due to their tiny tips (diameters around 1-20 μm) and high spatial resolutions, can meet such a special requirement and enable us to directly study distributions of chemical species and biochemical activities in micro-environment. Oxygen microelectrode, the most mature technique among microelectrodes developed so far, has played an important role in biofilm studies. There are two groups of oxygen microelectrodes, the separate and the combined. Most of previous research studies on DO in biofilms were based upon the application of the separate oxygen microelectrode that is more subject to interference from external environment. In comparison, the combined oxygen microelectrode, especially the one with a guard cathode initially developed for other

research areas, such as limnology and oceanography etc., is less sensitive to external interference. Consequently, it is more suitable for field measurements. However, this type of oxygen microelectrode is much more difficult to fabricate in laboratory than the separate type.

As a result, this project had two major objectives. The first was to explore the feasibility of conducting *in-situ* DO observation in wastewater biofilms directly in the field rather than in the laboratory by adopting the newly developed combined oxygen microelectrode. The second objective was to collect experimental evidence under field conditions to verify some conclusions on DO penetration in wastewater biofilms previously made on the basis of laboratory observations.

Due to the popularity and availability of the rotating biological contactor (RBC) system, two domestic wastewater treatment plants using RBC systems were selected in the Province of Alberta, Canada for this project. In order to conduct DO measurements in wastewater biofilms directly in the field, besides the combined oxygen microelectrode, a special setup for field DO measurements in wastewater biofilms was designed as well in this study. Using these apparatus, DO concentration profiles in wastewater biofilms were measured directly on RBC discs at these two sites. On the basis of these *in-situ* data, DO penetration depth and oxygen flux into domestic wastewater biofilms were determined.

In the following two chapters (Chapter 2 and Chapter 3) of this thesis, laboratory fabrication and evaluation of the oxygen microelectrode and the field study on DO penetration in wastewater biofilms are introduced in detail.

In Chapter 2, the theory and the history of oxygen microelectrode are first

introduced. Followed is a detailed description of the fabrication technique of the most advanced combined oxygen microelectrode with a guard cathode which was used in the field study. In the last part of Chapter 2, an evaluation of the fabricated oxygen microelectrode and its fabrication technique is discussed.

After the fabrication and evaluation of the oxygen microelectrode in the laboratory, a field study on *in-situ* DO measurement in wastewater biofilms was conducted by applying this fabricated oxygen microelectrode. Details about this field study are introduced in Chapter 3. Background of the two sites of our field study and the reason why they were selected as our study subject are provided in the first part of Chapter 3. Followed are the materials and methods used in this field study. Introduced next is the most important part - the results and discussions of this field study. In this part, DO profiles in wastewater biofilms have been constructed based on these *in-situ* data collected in the fields. Meanwhile, DO penetration depth and oxygen flux into wastewater biofilms are estimated on the basis of these constructed DO profiles. More detailed discussions on DO penetration depth and oxygen flux into wastewater biofilms are also provided in this part.

In the last part of this thesis (Chapter 4) are some major conclusions drawn from the results of this project and some recommendations for future work.

Chapter 2 Fabrication and Evaluation of Oxygen Microelectrode

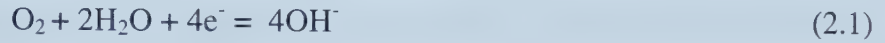
Based on a similar principle, various types of oxygen microelectrodes have been developed with various fabrication techniques in the past decades. These oxygen microelectrodes have their own advantages and disadvantages, but they generally can be classified into two groups. In order to fulfill our goal of conducting *in-situ* DO measurement in wastewater biofilms under field conditions, a newly developed oxygen microelectrode had been successfully fabricated in our laboratory for this project and was later used in the field study on DO penetration in wastewater biofilms.

In this chapter, the theory of the oxygen microelectrode is explained in the first section. In the second section, the history of the development of various fabrication techniques of the oxygen microelectrode is introduced. Described in the third section is a fabrication protocol, developed in our laboratory, for a combined oxygen microelectrode with a guard cathode. Finally, an evaluation is made for the oxygen microelectrode fabricated in the laboratory.

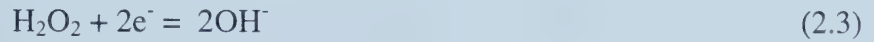
2.1 Theory of oxygen microelectrode

An oxygen microelectrode is an electrochemical device whose normal function is based on the reduction of oxygen on the surface of its cathode (the working electrode). Connected with the negative pole of an applied external voltage, the cathode, which is made from a material such as platinum or gold, which is chemically

less active, provides the oxygen molecule with electrons, hence makes it reduced on the surface of the cathode. The chemical reaction may be expressed by the following equation (Heineman, 1989):



The above reaction may be separated into two processes:



In many samples to be measured, there often exist other electro-active species reducible at the same potential and/or surface-active species adsorbable on the cathode surface, which could inhibit the reduction of oxygen. Therefore, an oxygen-permeable membrane is sometimes used in oxygen microelectrode. As a result, DO in the sample has to diffuse through the membrane and electrolyte between the membrane and the cathode before it is reduced on the cathode surface.

As a polarographic detector, when external voltages are applied to it, oxygen microelectrode can reach a limiting current appearing as a plateau in the current-voltage curve, as shown in Figure 2.1. The specific value of the voltage that provides a limiting current, known as polarization voltage, varies with the type of material used for the cathode. When a polarization voltage is applied and hence a limiting current is obtained, the reaction rate of oxygen reduction is fast and there is little or no oxygen accumulation on the cathode surface. The voltage variations within the polarization

voltage range corresponding to the current plateau have theoretically no impact on the current signal. Therefore, the reaction rate is only limited by oxygen diffusion rate from the sample to the cathode surface. Consequently, the limiting current is linearly proportional to the oxygen partial pressure (or activity) in contact with external surface of the membrane. This proportionality may be expressed by the following equation,

$$I = nFAS_mD_mP_{O_2}/Z_m \quad (2.4)$$

Where, I is current; n , number of electrons involved in reduction reaction; F , Farady constant; A , cathode area; P_{O_2} , oxygen partial pressure; Z_m , membrane thickness; S_m and D_m , solubility coefficient and diffusion coefficient of oxygen in the membrane, respectively (Hitchman,1983).

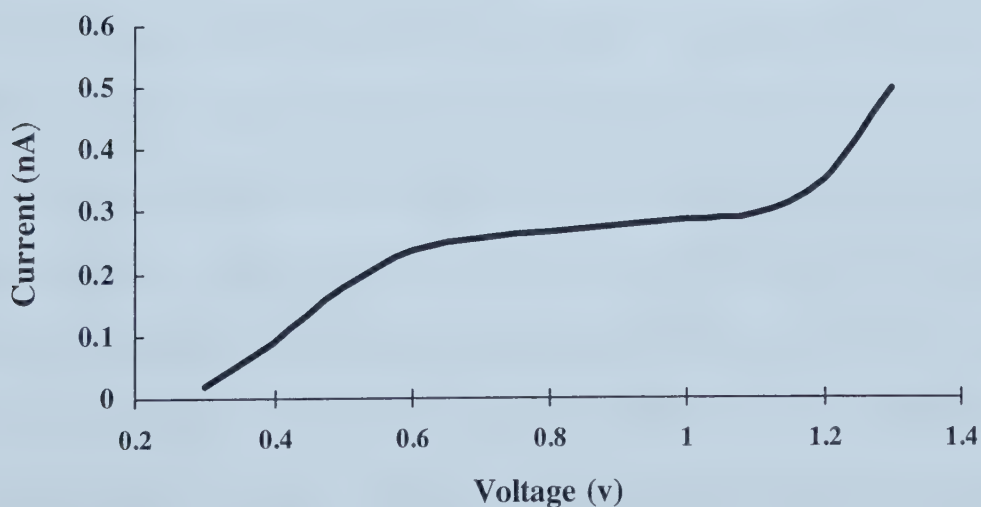


Figure 2.1 Current-voltage curve (Modified from Baumgärtl and Lübbers, 1983)

For a specific oxygen microelectrode, all terms on the right side of equation (2.4) are constants except for P_{O_2} . All these constant terms may be considered into a calibration factor that can be determined by calibration process before conducting sample measurement. In the calibration process, using standard water with known oxygen concentration (or partial pressure), a calibration curve can be constructed that can be used for sample measurement.

2.2 Development of oxygen microelectrode

The oxygen microelectrode has existed for several decades. The first oxygen microelectrode was developed in the 1940s. It was developed initially for medical research rather than environmental biofilms. The applications in environmental biofilms started in the late 1960s. There are basically two groups of oxygen microelectrodes: the separate and the combined. In the first group, an external reference electrode is needed for measurement, while in the second, there is an internal reference electrode integrated with the working electrode in the microelectrode.

An oxygen microelectrode is primarily used for measurement of conditions in a microenvironment, such as biofilms. In order to avoid disturbance to the oxygen conditions in the measurement, a very small tip (at micrometer scale) of the oxygen microelectrode is required. The current signal measured in the microenvironment is usually very weak and variable. Therefore, an oxygen microelectrode with special characteristics has to be fabricated. These characteristics include short response time, stable signals, low sensitivity to external interference, easy fabrication, increased

longevity, and less drifting effects. In order to meet these requirements, the fabrication techniques of the oxygen microelectrode, including the selection of the materials and the design of the fabrication procedure, are very critical. In the following sections, a detailed introduction to the development of the fabrication techniques for both the separate and the combined oxygen microelectrodes is given in the first two sections. A comparison between the separate and the combined oxygen microelectrode is made in the last section.

2.2.1 The separate oxygen microelectrode

A separate oxygen microelectrode serves as the working electrode during the measurement of oxygen concentrations, while a separate micro- or milli-reference electrode, usually a silver/silver chloride or calomel reference electrode, is needed to be placed in proximity. The external liquid between these two electrodes serves as electrolyte.

As early as 1942, a recessed platinum oxygen microelectrode (200 μm tip diameter) was developed by Davies and Brink (1942) to carry out the first correct oxygen tension measurement in animal tissues. A decade later, Dowben and Rose (1953) made an oxygen microelectrode using an alloy of 50% indium and 50% of tin (melting point 110°C). This alloy, as well as many other gallium and indium alloys, possesses the attractive property of "wetting" glass. This kind of property made it much easier to fabricate the microelectrode. After being melted on a hot plate, the alloy was drawn into a glass capillary by means of gentle suction. After cooling

down, a layer of gold and then a layer of platinum were electro-deposited onto the surface of the alloy. Different types of oxygen microelectrodes using different metals including platinum, gold, stainless steel, stainless coated with gold, antimony, and a platinum (90%)-iridium (10%) alloy were summarized by Cater and Silver (1961). All these oxygen microelectrodes were used for the measurement of oxygen tension in blood and tissues in the early days.

On the basis of Dowben and Rose's method, Whalen *et al.* (1967) described the fabrication and evaluation of the first low melting point alloy-filled oxygen microelectrode. They used the Wood's metal - an alloy with very low melting point (50% bismuth, 26.7% lead, 13.3% tin, and 10% cadmium, melting point 73-75°C) mixed with 6-10% (w/w) gold powder. The mixture was filled into a glass capillary such that a recess was formed at the tip of the microelectrode. The alloy surface at the tip was then electroplated with a layer of gold. Since the gold surface at the tip of the oxygen cathode microelectrode consumes little oxygen, this microelectrode does not require stirring of the sample to be measured. Meanwhile, this oxygen microelectrode was insensitive to stirring, which often exists in the media to be measured. This technique was soon applied to the studies of environmental biofilms (Whalen *et al.*, 1969; Bungay *et al.*, 1969; Bungay and Harold, 1971; Chen and Bungay, 1981; Bungay and Chen, 1981).

Whalen's method was further improved by Linsenmeier and Yancey (1987). They used a bismuth alloy (44.7% bismuth, 22.6% lead, 19.1% indium, 8.3% tin, and 5.3% cadmium, melting point 47°C). This alloy has a smaller volume increase (linear growth after solidification, 0.05%) than that of the Wood's metal (0.6%). The use of

this alloy reduced the occurrence of cracks in the glass, resulting from the expansion of the alloy after it was cooled down in the micropipette, and therefore improved the success rate of the fabrication and the longevity of the microelectrode. In their simplified procedure, there was no need to clean glass, to pull the alloy-filled glass micropipette, or to etch away the alloy from the tip. These modifications made the fabrication of oxygen cathode microelectrodes much easier. Fu (1993), Zhang (1994) and Yu (2000) applied this modified method to their studies on wastewater biofilms.

Inspired by the design of a membrane covering the tip of microelectrode to avoid influences from external media in a coaxial needle oxygen microelectrode (Baumgärtl and Lübbers, 1973, 1983), Revsbech (1983) developed a new separate oxygen microelectrode modified for oxygen analysis of sediments, which is called "Cathode-type oxygen microelectrode" (Revsbech and Jørgensen, 1986). In this microelectrode, a 0.1mm platinum wire was electrically etched, in KCN solution with 2-7 V AC applied, to a diameter of 1-4 μm at the tip and then inserted into a pre-cleaned thin-walled soda-lime capillary (AR-glass). The etched platinum wire was then coated with the glass at the tip by hanging the capillary vertically through an electrically heated nichrome loop. When the glass melted, gravity pulled the platinum wire through the melting zone and a thin glass coating was produced. Afterwards, the extreme tip of the platinum wire was exposed by grinding off excess glass on a rotating disc covered with 0.25 μm grain size diamond paste. After grinding, the tip of the platinum wire was etched briefly in KCN solution so that a 5-10 μm long recess was formed. In the recess, the platinum tip was then coated with gold by electroplating using 5% $\text{KAu}(\text{CN})_2$ solution. Finally, the tip of the electrode was

covered with a double membrane of collodion and polystyrene, which avoids problems with rapid poisoning of the precious metal surface. The microelectrode provided relatively good spatial resolutions and had a response time not exceeding 2 seconds. This design became a solid basis for the later development of a much more popular combined oxygen microelectrode that can overcome some major problems associated with the Cathode-type oxygen microelectrode.

Nishidome and Kusuda (1988) developed another way to fabricate a separate oxygen microelectrode. They used a piece of Ag-coated Pt wire (length: 6 cm, diameter: Ag 100 μm , Pt 15 μm). One end (2 cm in length) of this wire was dipped in concentrated nitric acid to expose the inner Pt wire. Meanwhile, a glass tube (OD 2 mm, ID 0.8 mm) was drawn over a gas burner to narrow its tip to an inner diameter of 15 μm . Afterwards, the Pt wire was inserted into the glass tube under microscope to make sure that both tips are in close contact. Then both tips were melted together over a gentle flame. The other end of the Pt wire was soldered to a lead wire that was connected to a voltage detector. This type of oxygen microelectrode was employed in some research work on wastewater biofilms in Japan (Nishidome and Kusuda, 1988; Nishidome *et al.*, 1994).

2.2.2 The combined oxygen microelectrode

In a combined oxygen microelectrode, both the working and reference electrodes are integrated in one body of a microelectrode. There is no need for external solution serving as electrolyte.

The first combined oxygen electrode was invented by Clark (1953) for the measurement of oxygen tensions in blood. It was not a microelectrode but the basic concept is preserved in the later microelectrode models. In this Clark-type electrode, both the sensing electrode (the cathode: platinum wire) and the reference electrode (the anode: silver wire) were integrated in one electrode, both standing in parallel inside a capillary. In addition, the tip of this electrode was covered with an oxygen permeable membrane, which could protect the platinum cathode from direct contact with the blood samples and also minimize the electromagnetic interference. This electrode requires stirring of the sample to maintain a stable oxygen concentration because the reduction of oxygen at the platinum surface consumes oxygen at a rate slightly higher than the diffusion rate through viscous fluids.

This Clark-type electrode had some disadvantages. First of all, the cathode itself could not be made smaller than about 25 μ m. This made the casing even bigger, and the sensor would then be less suitable to measurements of micro-scale oxygen gradients. Secondly, the response time was relatively slow (e.g. 1 minute) as the oxygen had to diffuse through the rather thick membrane, and furthermore the sensor was sensitive to stirring. Finally, the Clark-type electrode exhibited aging effects (Ferris, 1974).

Baumgärtl and Lübbers (1973,1983) described a coaxial needle oxygen microelectrode, used for the measurement of oxygen tensions in tissues. In their procedure, a fine platinum wire was etched and fused into a glass capillary. A layer of gold was electroplated onto the surface of the platinum tip to form the cathode. In comparison to platinum as a cathode material, gold has much wider polarization

voltage range (-0.5 V to -1.2 V) than platinum (-0.5 V to -0.85 V) that appears as a broader plateau in a current-potential curve. The gold layer also enlarges the cathode surface by its fine granular structure and produces a signal distinctly higher than that of the platinum surface (Baumgärtl and Lübbers, 1983). The shaft of the cathode was then coated with multiple thin layers of tantalum/platinum/silver. The tantalum layer sticks well to the glass surface, while the intermediate platinum layer guarantees a good electrical conductivity. A thin layer of silver chloride, developed from the silver layer, shields the platinum wire inside the microelectrode from electrical noise, and at the same time, it serves as the reference microelectrode. The tip of the microelectrode was then covered with a layer of nontoxic, oxygen permeable membrane. A systematic investigation of the properties of this coaxial needle oxygen microelectrode is available in Baumgärtl (1987). This type of oxygen microelectrode was used in a number of studies on oxygen supply in tissues and micro-circulation of blood (Baumgärtl and Lübbers, 1983). It was also used in the early studies of marine sediments (Revsbech *et al.*, 1980, 1983).

On the basis of the coaxial needle oxygen microelectrode and the Cathode-type oxygen microelectrode, Revsbech and Ward (1983) later developed the Clark-type electrode into a micro-scale electrode, which is called "Clark-type oxygen microelectrode" (Revsbech and Jørgensen, 1986). This microelectrode was used for the measurement of oxygen in marine sediments and other natural media (Revsbech and Ward, 1983; Kuenen *et al.*, 1986; Revsbech and Jørgensen, 1986). In this microelectrode, both the sensing and reference microelectrodes were situated in parallel inside a casing glass capillary, with the tip of the reference electrode behind

that of the sensing electrode. The fabrication process of the sensing cathode was almost the same as described by Revsbech (1983) for the separate oxygen microelectrode (the Cathode-type). The only difference is in the tip structure. Previously, the glass-coated platinum tip was naked and then etched to get a recess within the coating glass for gold plating. While here the glass-coated platinum wire was naked at the tip and then the exposed platinum was directly electro-plated with gold. The outer glass casing of the Clark-type microelectrode was also made from soda-lime glass and had been initially shaped, especially at its very tip, with a microforge. The sensing electrode was then inserted into this casing with a micromanipulator and a partial seal between the casing and the sensing electrode was made with fast-curing epoxy. The silicone rubber membrane that is oxygen permeable was applied by introducing the tip of the electrode into uncured silicone rubber. After the silicone rubber totally cured, the electrode was then filled with an electrolyte solution. Finally, the AgCl-covered silver wire was introduced into the electrolyte to form the reference electrode.

In order to obtain much more stable measurement, Revsbech (1989) modified some parts of the Clark-type oxygen microelectrode and developed a new fabrication technique. In this newly developed combined oxygen microelectrode, the most important modification is the addition of an internal auxiliary electrode (tapered silver wire) as the guard cathode integrated with the sensing and the reference electrodes in one small glass capillary. This guard cathode can remove 99.999% of oxygen radially diffusing toward the sensing tip from the internal electrolyte solution (Hitchman, 1983). This is particularly important when exposed to anoxic environment, because

this kind of configuration can ensure a reasonably low residual (zero) current for measurement hence much more accurate readings. This configuration also allows the current to flow internally, so the membrane does not have to be a part of the circuit. Furthermore, the internal electrolyte can also serve as an electrical shielding of the sensing electrode. Such a new integrated structure makes much more accurate measurements possible in biofilms because high level of stirring effects often existing during measuring can be greatly reduced.

Another modification in this new microelectrode is the outermost 3-4 cm of the shaft of the sensing electrode. This part was made from the green glass (Schott 8533), even though the remaining part of the shaft was still made from the same material as used in the "Clark-type oxygen microelectrode" - soda-lime glass. This green glass is lead-free and has low melting point, high alkaline resistance and low conductance toward the electrolyte. After having been inserted with the etched platinum wire, the green glass was fused tightly with the sensing electrode shaft of the soda-lime glass. This modification can greatly reduce the likelihood of the damage of the etched platinum tip during fabrication process.

Because of the introduction of the guard cathode, the outer casing of this new microelectrode has to be made very wide compared to the sensing electrode. This will allow sedimentation of particulate materials ("dirt") to the tip of the microelectrode. Such deposits cause noise in measuring. In order to avoid this problem, a few milligrams of 30-60 μm glass beads was added, which can efficiently block small particles before they reach the tip.

The use of such a unique combined oxygen microelectrode with smaller

diameters has greatly improved the capability for repetitive measurement and increased the versatility of the microelectrode technique in biofilm studies (Rasmussen and Lewandowski, 1998a,b; Santegoeds *et al.*, 1998; deBeer and Schramm, 1999).

2.2.3 Comparisons of oxygen microelectrodes

By reviewing the applications of oxygen microelectrodes in past years, it can be seen that the separate oxygen microelectrode still has been used a lot even after the advent of the more advanced combined oxygen microelectrode. This is because each of these two types of microelectrodes has its own advantages and disadvantages, which should be evaluated based upon their applications. A comparison between these two oxygen microelectrodes is summarized in Table 2.1.

Within the group of combined oxygen microelectrode, the one with a guard cathode is the best in terms of performance. A shorter history of this unique oxygen microelectrode is one of the major reasons for its rare applications in the research area of environmental biofilms. However, the difficulty in its fabrication is another major reason. For laboratory study, the use of separate oxygen microelectrode can often be adequate. This is because separate oxygen microelectrode is relatively easy to fabricate and the experimental conditions in the laboratories can often be controlled. For field study, however, the combined oxygen microelectrode with a guard cathode is obviously more advantageous in terms of stability, precision and accuracy of reading in measurements.

Table 2.1 Comparisons of oxygen microelectrodes

Item	The separate oxygen microelectrode	The combined oxygen microelectrode
Fabrication	Relatively easy	More difficult
Vulnerability to external electromagnetic interference	Very vulnerable	Much less vulnerable
Requirement for external media	High electrical conductivity	No such special requirements
Sensitivity to temperature changes	Sensitive	Less sensitive
Reliability/stability of reading	Low	High
Chemical poisoning from media	Rapid to tips of those without membrane covering	Very rare
Sensitivity to stirring effect	Sensitive	Less sensitive
Response time	Less than 2 seconds	Less than 2 seconds

2.3 Fabrication of oxygen microelectrode

This research project was to conduct *in-situ* DO measurement in wastewater biofilms directly under field conditions, where more potential interference on oxygen microelectrode might exist and sometimes are out of our control. Consequently, in order to avoid and/or reduce such interference, the combined oxygen microelectrode with a guard cathode was selected in this project. The fabrication of this type of oxygen microelectrode is introduced in the following sections. In principle, the

fabrication procedure follows Revsbech's design (1989), but many practical details and some modifications are mainly based on our own laboratory experience.

The structure of the combined oxygen microelectrode with a guard cathode is illustrated in Figure 2.2. It comprises a working cathode with glass shaft, a reference electrode, a guard cathode, the outer casing, the electrolyte and the oxygen permeable membrane.

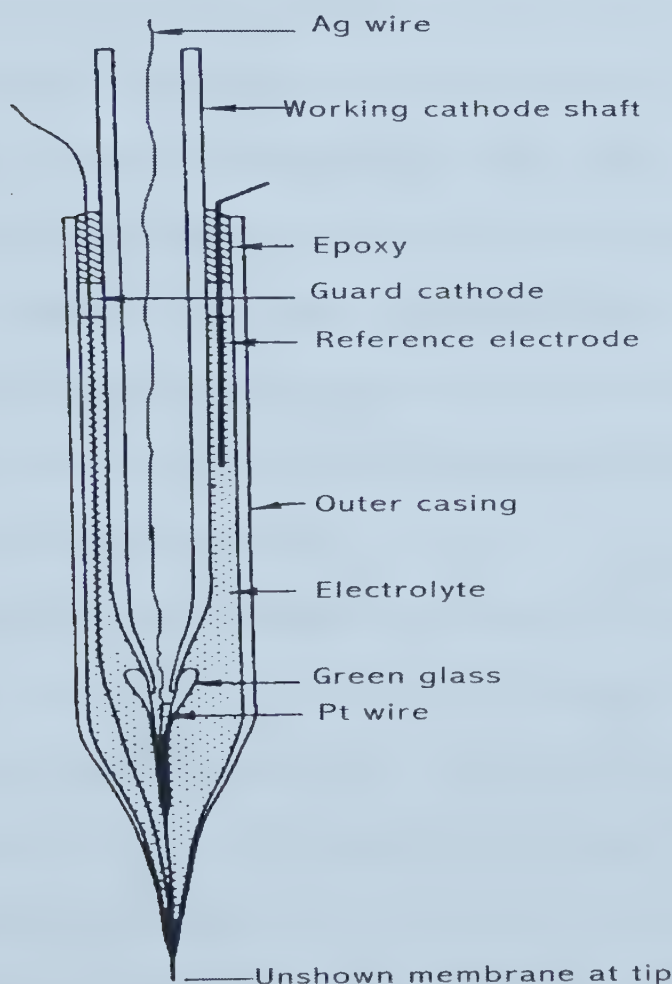


Figure 2.2 Schematic diagram of a combined oxygen microelectrode with a guard cathode (Modified from Revesbech, 1989)

Preparation of the working cathode shaft. This glass shaft consists of two parts: the white tubing (Schott Glas Export GmbH, Mainz, Germany; Schott 8350, outer diameter: 4.0 mm; wall: 0.5 mm) and the green tubing (Schott 8533, outer diameter: 3.33 mm, inner diameter: 2.69 mm). Glass tubing with 15 cm in length for both glasses were cleaned with 0.1M HCl and deionized water and dried in oven at 103°C. After being cooled down, the glass tubing for both glasses were heated, one at a time, at the middle section over a natural gas burner. When the middle section became very soft, the glass tubing was taken out of the flame and simultaneously pulled by both hands until the middle section became around 2.5 mm in diameter for the white glass or a very fine capillary for the green glass. These pulled glass tubes were cut in the middle. For the green glass tubing, its un-pulled end was further cut off such that only about 2 cm of un-pulled tubing was left. Finally, the pulled end of the white tubing was inserted into the un-pulled end of the green capillary and their joint was melted together over a butane burner (Bernzomatic, NY, USA; Micro Torch, Model No. ST1000TS) with a fine flame.

Etching of the working cathode wire. A piece of Pt wire (Aldrich Chem. Co., Milwaukee, WI, USA; Cat. No. 35,736-7; 99.99%, diameter: 0.10 mm, length: about 6 cm) was soldered with a piece of Ag wire (Aldrich Chem. Co., Milwaukee, WI, USA; Cat. No. 32,703-4; 99.99%, diameter: 0.25 mm, length: 15 cm). Then, in a well-ventilated fume hood, the tip of the Pt wire (about 1cm in length) was etched in 1M KCN solution (in a small beaker) under 6-7 V voltage, supplied from the Power supplier. The power supplier consists of a fixed transformer (Hammond Manufacturing, Canada; Model No. 167S12; Primary: 115 V, Secondary: 12.6 V, 10A)

and an adjustable transformer (The Superior Electric Co., Bristol, Connecticut, USA; type 116), in series, with the Pt wire as one electrode and a graphite rod as the other. The Pt wire was kept being moved up and down for several minutes during this etching process until a tip diameter as small as 1-2 μm was obtained. Then, the etched Pt wire was cleaned by being immersed, in turn, in three 250 mL beakers of deionized water. Finally, this etched Pt wire, soldered with Ag wire, was gently inserted into the fore-prepared working cathode shaft with the etched Pt wire staying in the green capillary.

Tapering of the working cathode tip. First, two stands were prepared: an adjustable stand for micromanipulator installation and a normal extension clamp stand for holding a porcelain socket fixed with a piece of W-shaped canthal wire as a heating loop. Then, the working cathode shaft was hung from its capillary end by using a small clip mounted on the micromanipulator (World Precision Instruments, Inc., Sarasota, FL, USA; Model M3301R). This setup was adjusted such that the capillary section of the working cathode shaft was placed in the W-shaped heating loop with the tip of the etched Pt wire within the capillary located at about 2-3cm above the heating loop, as shown in Figure 2.3. Heat was then provided by gradually turning up the power supplier until the glass capillary started melting. Once the glass capillary was slowly dropping down (due to melting) to a point where the tip of the etched Pt wire was about 0.5-1 cm above the heating loop, the voltage was quickly increased so as to make the melting glass less viscous, thus coating on the Pt wire. Finally, the whole cathode shaft dropped into a beaker underneath, with napkins on its bottom. The whole process was monitored under a horizontal microscope (Carl Zeiss,

Jena, Germany; Model Stemi SV11). The tapered working cathode was fixed with a one-hole rubber cork and inserted into a test tube for temporary storage.

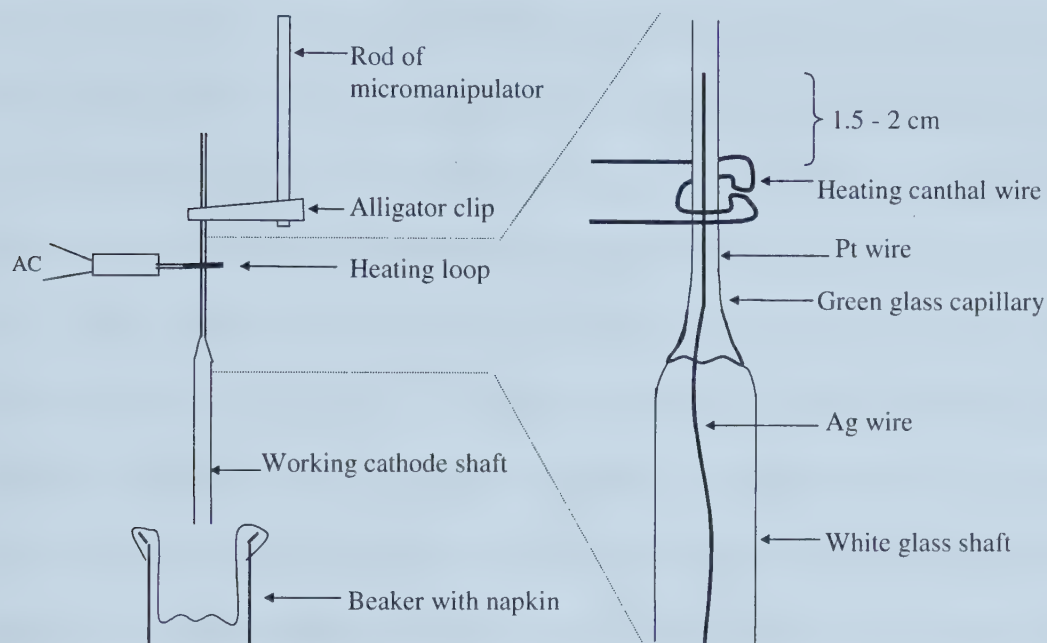


Figure 2.3 Schematic diagram for tapering of the working cathode tip

Gold-plating of the working cathode tip. A gold-plating circuit was prepared by first connecting the negative pole of a 1.5 V battery to the Ag wire in the working cathode shaft. The positive pole of the same battery was then connected, in series, with an adjustable resistor (Duncan Electronics Inc., California, USA; Model 3253, 0-200 Ω); a piece of Ag wire (99.99%; diameter:0.25 mm), and a short piece of Pt wire that was inserted into the large end of a Pasteur pipette. The other end of this Pt wire was immersed in the AuCl_3 solution (around 0.1M) (Fisher Scientific, G54-1;

$\text{HAuCl}_4 \cdot 3\text{H}_2\text{O}$, FW=393.83) which had been sucked in the tip of the Pasteur pipette. The glass coating over the tip of the tapered working cathode was removed by using a micro-dissecting tweezer (Roboz Surgical Instrument Co., Inc., Rockville, MD, USA; Cat. No. RS-4905). This step was conducted carefully under a vertical microscope with built-in scale (Carl Zeiss, Model: Axioskop 2 Plus). During the plating process, the naked cathode tip was advanced, through the movement of the microscope stage, into the AuCl_3 solution and stayed there for several seconds under a voltage of around 0.8 V, which was obtained by adjusting the adjustable resistor. The result of the plating process was a layer of electro-plated gold on the naked cathode tip. The ultimate gold-plated tip had a diameter as small as several micrometers. The gold-plated working cathode was then fixed with a one-hole rubber cork and inserted into a test tube for temporary storage. Here, the length of time that the actual process lasts is determined by the concentration of the AuCl_3 solution and the voltage applied. Generally, any combination of them is acceptable as long as it provides a process that produces the needed gold layer and is easy to control, which means a longer plating time. Based upon our experience, it is better to use a relatively dilute AuCl_3 solution. In this case, this gold-plating process will take a longer period of time instead of only several seconds. As a result, this process can be controlled more easily.

Preparation of the outer casing. The fine section (specific location dependent on the ultimate length of the microelectrode) of a cleaned Pasteur pipette was heated over the natural gas burner and then pulled by hands until a diameter around 0.5 mm was obtained. Then the pulled pipette was hung with its fine end clipped in the micromanipulator and its pulled part placed in the W-shaped heating

loop. The pipette was heated by gradually turning up the power supplier until the glass started melting. As the pipette started dropping, it was kept being moved upwards slowly so as to obtain a suitable length and diameter of the casing tip. Finally, the casing dropped into the beaker underneath, with napkins on its bottom. The ultimate diameter of the casing tip was determined according to the tip size of the gold-plated cathode at the following assembly stage. The tapered outer casing was fixed with a one-hole rubber cork and inserted into a test tube for temporary storage.

Preparation of the guard cathode. A cleaned white glass tubing was heated over the natural gas burner and pulled straightforward by hands until an inner diameter bigger than the Ag wire (Aldrich Chem. Co., Milwaukee, WI, USA, Cat. No. 26,555-1; diameter: 0.127 mm) was obtained. The pulled capillary was then cut into 7-8 cm long sections. A piece of the Ag wire with a length of about 20 cm was inserted into the fore-prepared capillary with its two ends extending out of the capillary. One end of the capillary was sealed with Epoxy (Mastercraft Canada, Toronto; 5 minute Epoxy, Resin & Hardener) and then was dried in the air. Afterwards, in the fume hood, the tip (about 1cm in length) of the sealed Ag wire was etched in 0.5M alkaline KCN solution until a diameter around 1-5 μm was obtained. Except for using Ag rather than Pt wire as one electrode here, the whole etching process was similar to that for Pt wire of the working cathode.

Preparation of the reference electrode. A piece of the Ag wire (diameter: 0.25 mm) was connected to the negative pole of a 1.5V AA battery and another piece of the same Ag wire (about 8 cm in length) with the positive pole of the same battery. Then both of these Ag wires (about 3-4 cm in length) were immersed in 1N HCl

solution in a small beaker. In about 1-2 minutes, the color of the immersed section of the Ag wire connected with the positive pole became brown, which is the color of AgCl. This AgCl-covered Ag wire was then rinsed with deionized water and later served as the Ag/AgCl reference microelectrode.

Assembly of the oxygen microelectrode. The outer casing was fixed on the microscope stage. The working cathode, cleaned with ethanol, was inserted into the outer casing and pushed carefully toward the tip of the outer casing by using the micromanipulator. The distance between the tips of the working cathode and the outer casing was controlled at about 30 - 50 μm . If the distance was too long, a micro dissecting tweezer could be used to cut the outer casing tip short. Another option could be to use a tip-closed Pasteur pipette, mounted on a micromanipulator, to bump the tip of the outer casing to break it short. The shaft of the working cathode was then fastened on the stage of the microscope by the spring clip on the stage. Afterwards, the guard cathode was inserted along the working cathode but stopped behind its tip. Finally, the reference electrode was inserted into the outer casing so that its brown section was kept just within the outer casing. Epoxy was applied to glue these working, guard and reference electrodes with the outer casing, but an open space between these electrodes and the outer casing was still kept here for future addition of electrolyte and glass beads. A tip-closed Pasteur pipette covered with silicone (Dow Corning Co., MI, USA; Silastic Medical Adhesive, Type A, Content sterile) at its tip was mounted on the micromanipulator and was located such that its silicone-covered tip exactly pointed toward the outer casing tip. Then the pipette tip was moved toward the outer casing tip by adjusting the micromanipulator so as to get a membrane with a

thickness of 10 - 20 μm within the outer casing tip. The half-finished microelectrode was then fixed with a one-hole rubber cork and stored in a test tube overnight to dry the Epoxy and the silicone membrane in the air. Before electrolyte was injected into the outer casing, the open end of the working cathode shaft was sealed with Epoxy with the Ag wire still extending out of the shaft. This can help reduce the likelihood of electrolyte leakage at the shaft joint. Afterwards, a little electrolyte (a mixture of 0.2M KHCO_3 (50 ml), 0.3M K_2CO_3 (50 ml), 1.0M KCl (100 ml) and thymol (a little) was first injected into the assembled outer casing, using 1mL syringe (Becton Dickinson & Co., Franklin Lakes, NJ, USA; Recorder No. 309597) with a filter device (Fisher Scientific, Cat. No. 5-713-401; Puradisc 25PP, Whatman, 0.2 μm). Then the outer casing was checked under microscope to see if there was any air bubble(s) within it, especially in the tip part. If there was, then the tip was immersed into a beaker of degassed water (obtained by boiling water for several minutes) to eliminate bubble(s). After bubbles were eliminated, a very small amount of glass beads (3M Empore, St. Paul, MN, USA; Filter Aid 400; diameter: 20-40 μm ;) was added into the outer casing and electrolyte was further injected until the outer casing was full. Finally, Epoxy was applied to completely seal the outer casing and then was dried in the air.

Preparation of connecting cables and connectors. For the working cathode, a shielded cable (RG174) was used to connect at one end with a BNC crimp type connector (for RG 174) and the other with a small alligator clip. For the guard cathode and reference electrode, unshielded, plastic-covered copper cable was used to connect at one end with a banana plug and the other with an alligator clip.

2.4 Evaluation of oxygen microelectrode

The major purposes of this evaluation process were: (1) to verify that the above fabrication procedure was effective; (2) to confirm that every step of this designed fabrication procedure was carried out correctly; (3) to demonstrate that the oxygen microelectrode to be used for real measurement was in good condition; and (4) to obtain the calibration curve for the specific oxygen microelectrode.

The evaluation of the oxygen microelectrode was made on the base of the following two processes: polarization and calibration. The parameters used for the evaluation of the oxygen microelectrode included the current signals under oxygen-free and air-saturated conditions, the difference between these two extreme signals, the linearity of the calibration curve, the residual current signal, the stirring effect, and the response time.

2.4.1 Polarization and calibration methods

The proportionality between current signal and oxygen partial pressure in a sample is valid only when oxygen reduction rate on the working electrode surface is oxygen-diffusion-limited from outside of the membrane. Therefore, pre-existing oxygen in the electrolyte should be consumed first and a limiting current should be obtained through the polarization.

From equation (2.4), it can be concluded that the calibration factor for a specific oxygen microelectrode is unique. This is because some terms of the calibration factor, such as the cathode area (A) and the membrane thickness (Z_m), vary

from one microelectrode to another. Consequently, in order to establish the linear relationship between the current signal and oxygen partial pressure, the calibration factor has to be determined for a given oxygen microelectrode. The calibration factor is determined by measuring the current signals for two standard waters with known oxygen partial pressures or concentrations. Usually, one of the standard waters is oxygen-free and the other air-saturated. As a result, a two-point calibration curve is constructed, which then can be used for real sample measurement. The calibration factor is the slope of this calibration curve.

In our laboratory, the polarization and calibration for the oxygen microelectrode were conducted with a picoammeter (Unisense, Denmark, Model No. PA2000). Before starting the polarization, the polarization voltage was adjusted to -0.80 V on the picoammeter. Then the oxygen microelectrode was secured in a calibration chamber, with its tip immersed in distilled water. The calibration chamber was made of plexiglass with a volume of approximately 500 mL. The cap of the calibration chamber has three holes: one for the gas inlet tubing, the other two for two oxygen microelectrodes to be polarized simultaneously. When the polarization was initiated, the current signal was as high as 2.5 nA and then dropped very quickly in the first few minutes. The whole polarization process lasted overnight and a stable current readout was then achieved.

Although a calibration is conducted primarily for establishing a calibration curve, other parameters such as stirring effect (Re) and residual current of the oxygen microelectrode can also be obtained through a calibration process. In our laboratory, after the above polarization, the oxygen microelectrode was kept in the calibration

chamber, with its tip immersed the distilled water. Compressed air (21 % oxygen) or nitrogen gas (0 % oxygen) was vigorously flushed into the water through a gas dispersion tube with a flow rate without changing water temperature in the chamber during this calibration process. The readout from the picoammeter was continuously recorded every 20 seconds once the gas bubbling started. The calibration conditions were changed in the following sequence during the calibration process: start nitrogen flushing, stop nitrogen flushing, start air flushing, stop air flushing, repeat air flushing, stop air flushing and switch to nitrogen flushing simultaneously. The above sequence was repeated for duplication.

In addition to above two-point calibration (21 % and 0 % of oxygen), a third calibration point was also measured by flushing a mixed gas with 10.5% of oxygen balanced with nitrogen. The purpose was to check the linearity of the relationship between the current signal and the oxygen partial pressure for the oxygen microelectrode.

The test for response time of the oxygen microelectrode was also conducted before it was used for real sample measurement. In this test, the oxygen microelectrode was quickly switched from the oxygen-free condition to the air-saturated condition. The time the oxygen microelectrode needs to increase its readout from zero to 90 % of the value for air-saturated readout is recorded as the response time for this specific oxygen microelectrode.

2.4.2 Calibration results and discussions

The test results of the entire calibration process for the oxygen microelectrode are shown in Figure 2.4. The test data are listed in Appendix 2.1.

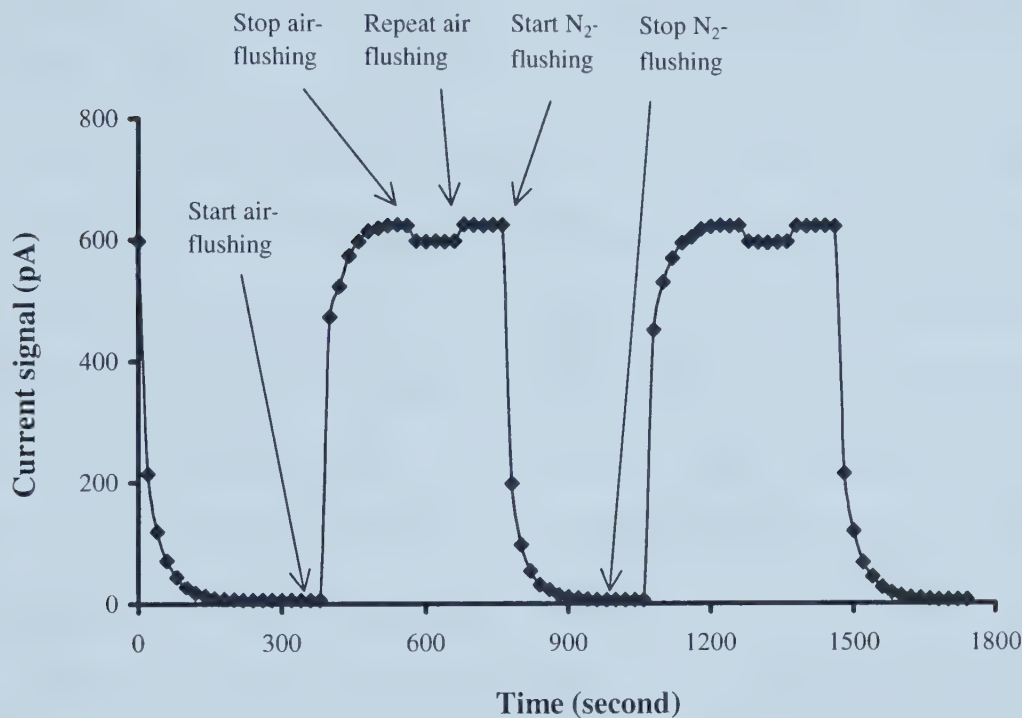


Figure 2.4 Calibration for an oxygen microelectrode

As shown in Figure 2.4, the current signal rapidly increased from the bottom (at 6 pA) to the peak (at 625 pA) within 2 minutes after the compressed air flushing was started. The peak signal was very stable at this level while the air flushing continued. After the air flushing was stopped, the signal dropped a little down to 599 pA and was stable at this level for minutes. After the air flushing was started again, the signal rebounded back to the initial peak level and remained at that level as the air

flushing continued. When the air flushing was stopped and, at the meantime, the nitrogen gas was flushed into the calibration chamber, the signal decreased very rapidly from its peak value down to the bottom (at 6 pA) within 3 minutes. As the nitrogen gas flushing continued, the signal was stable at the same low level. This was an entire circle of a calibration process. The duplication was conducted and is also illustrated in Figure 2.4.

The data from this calibration process show that the reading for the oxygen-free condition (6 pA), which was reached after nitrogen gas flushing, is about 1 % of the reading for the air-saturated condition (599 pA), which was reached after compressed air flushing and under stagnant water condition. Generally, the bigger the reading difference between these two conditions, the better the microelectrode is. From this perspective, this near 100 times difference between the two readings demonstrates that this oxygen microelectrode worked very well.

Based upon the three-point calibration (0 %, 10.5 % and 21 % of oxygen), a calibration curve is constructed in Figure 2.5. The data for this figure are listed in Appendix 2.2. As a result of linear regression, the high value of R^2 ($= 1$) was obtained. This has clearly shown a linear relationship between the current signal and the oxygen partial pressure of this oxygen microelectrode. This illustrates again that this oxygen microelectrode worked very well and can satisfy the requirements for DO measurements.

Generally, a concentration unit of mg/L is used for DO. The unit conversion from volume percentage (%) to mg/L is illustrated as the follows:

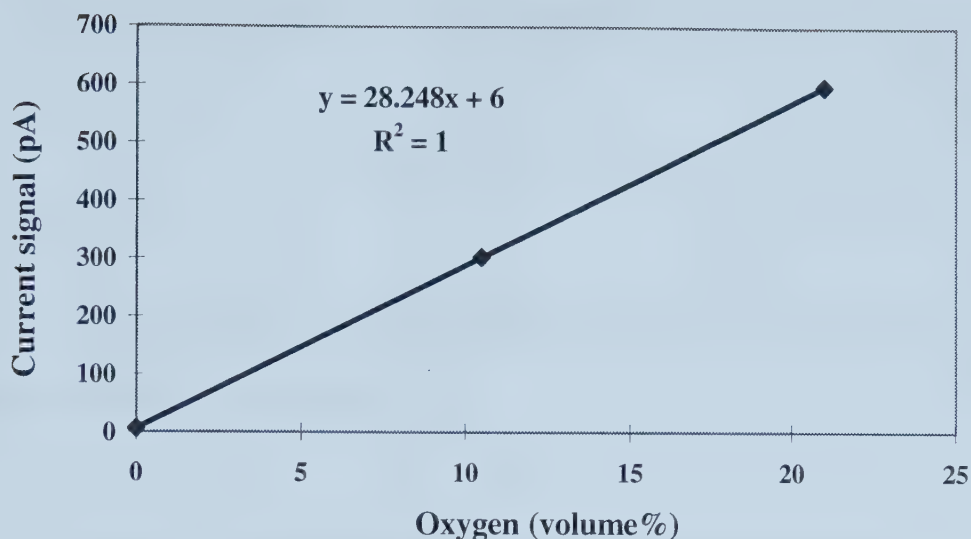


Figure 2.5 Calibration curve for an oxygen microelectrode (current signal vs oxygen volume fraction in dry calibration gas)

According to the calibration conditions (water temperature: 20°C, water salinity: 0 ‰ *), a value of 9.09 mg/L was selected from Table A in the “YSI MODEL 50B Dissolved Oxygen Meter Instruction”. This value is the solubility of oxygen in mg/L in water exposed to air at 760 mm Hg pressure. Then, according to the local altitude (668 m for Edmonton, Alberta), a correction factor of 92 % was selected from Table B in the “YSI MODEL 50B Dissolved Oxygen Meter Instruction”.

*: In our field study, all wastewater samples (raw and filtered) taken from each RBC stage at Devon and Olds were tested for salinity using a salinity meter (YSI Model 33 S-C-T Meter) (Yellow Springs Instruments Inc., Yellow Springs, Ohio, US). The results showed that salinities of all these wastewater samples were less than 0.5‰ which is negligible here. As a result, adoption of a zero value for salinity is comparable for both types of waters (distilled water in the calibration test and the domestic wastewater in real RBC biofilm DO measurement).

As a result, the corrected solubility of oxygen is calculated as the follows:

$$9.09 \text{ mg/L} \times 92 \% = 8.36 \text{ mg/L}$$

Results of oxygen unit conversion for all three points are listed in Table 2.2, which are the data for Figure 2.6.

Table 2.2 Results of oxygen unit conversion and data for Figure 2.6

Current signal * (pA)	O ₂ (volume %)	DO (mg/L)
6	0	0
303	10.5	4.20
599	21	8.36

* Reading under stagnant water.

For a normal sample measurement, generally a two-point calibration curve (0 % and 21 % oxygen) is sufficient. In a particular sample measurement, however, local atmospheric pressure (or altitude), salinity and temperature of the sample should be taken into consideration for such an oxygen unit conversion, and the calibration curve and DO value for real sample measurements should be constructed and determined accordingly.

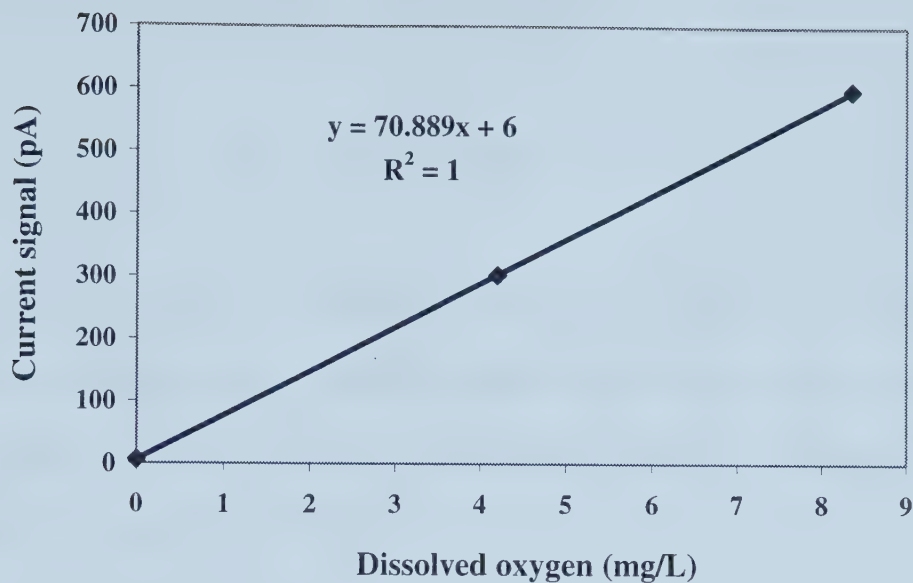


Figure 2.6 Calibration curve for an oxygen microelectrode (current signal vs dissolved oxygen concentration)

The lowest reading (6 pA) for the oxygen-free condition showed that the residual current of this oxygen microelectrode was not very high, although there are some aspects in design and fabrication that can be modified in the future to further reduce this residual current. These aspects include the glass selection, the size and shape of the gold-plated cathode tip, the distance between the membrane and the working cathode tip, the distance between the working cathode tip and the guard cathode.

During this calibration process, the stirring effect (Re) of this oxygen microelectrode was determined by switching the water condition from stirring (air-flushing) to stagnant (air-flushing stopped). The value of Re is calculated by using the

following formula (Baumgärtl and Lübbers, 1983):

$$Re = [(I - I_1)/I] \times 100\% \quad (2.5)$$

where I is the current under stirred air-saturated water and I_1 is the current under stagnant air-saturated water. For this specific oxygen microelectrode, the average values were used for the value of I (625 pA) and I_1 (599 pA). Therefore, the Re is calculated as follows:

$$Re = [(625 - 599)/625] \times 100\% = 4 \%$$

As a result, the stirring effect of this oxygen microelectrode is 4 %.

The response time of this oxygen microelectrode was tested to be less than 2 seconds. This is normally fast enough for DO measurement in wastewater biofilms, which generally are non-photosynthetic (Ward *et al.*, 1992). In the case of a photosynthetic biofilm, the oxygen concentration in the biofilm could vary more rapidly with a larger magnitude due to the synthetic reaction continuously occurring in the biofilm. As a result, a much shorter response time of the oxygen microelectrode is needed.

The response time, stirring effect, residual current and sometimes even tip size could all be important indexes in evaluating an oxygen microelectrode. The evaluation of a specific oxygen microelectrode should, however, be conducted with regard to its specific application. For example, a short response time could be crucial

in some applications. The short response time could be achieved by reducing the membrane thickness and/or the distance between the working cathode tip and the membrane. As a result, these measures would lead to increased stirring effect, which might be intolerable for the applications. Therefore, in real applications, reasonable and acceptable compromises often have to be made when weighing the above indexes. A balance could be achieved through modifications in the design and fabrication process.

In summary, the results of this evaluation process have indicated that the fabrication protocol for oxygen microelectrode is effective. The product of this fabrication protocol, the oxygen microelectrode, worked very well. As shown later in Chapter 3, the results of the field study have further proven that the oxygen microelectrode fabricated using this protocol was a reliable tool for *in-situ* DO measurement in wastewater biofilms under field conditions.

Chapter 3 Field Study on Oxygen Penetration in Wastewater Biofilms

3.1 Introduction

Biofilm reactors have been widely used in biological wastewater treatment. Oxygen acts as an electron acceptor in biochemical reactions occurring in wastewater biofilms. The concentration of DO plays a key role in the development of various microorganism communities, which in turn play different roles in substrate removal in wastewater treatment. As a result, a good understanding of DO in wastewater biofilms is essential for the rational optimization of biofilm reactor design and operation.

Biofilm, comprising cell clusters and voids, is a very complex environment, which is resistant to many of the traditional analytical techniques used in microbial ecology (Ward *et al.*, 1992). Therefore, tools with high spatial resolution on micro-scale are very crucial to biofilm studies. The oxygen microelectrode, due to its tiny tip (diameter at 1-20 μm) and high spatial resolution, can meet this special requirement and enable us to directly study the distribution of DO in wastewater biofilms.

Whalen *et al.* (1969) applied an oxygen microelectrode to the study of oxygen transfer in biofilms for the first time. They took natural biofilm samples from a polluted stream back to the laboratory for the study. The DO profile in the biofilm was determined using a separate oxygen microelectrode to directly measure the DO concentrations in the liquid and the biofilm. Each point on this DO profile reflects the equilibrium between the supply of oxygen through oxygen transfer into the biofilm and the utilization of oxygen through the microorganism activities in the biofilm. This

technique for the measurement of DO profile has later been widely employed in biofilm studies.

Bungay *et al.* (1969) determined oxygen diffusivity in the bulk water and the biofilm directly from the DO profile by applying the laws of diffusion. Williamson and McCarty (1976) developed the concept of diffusive boundary layer between the biofilm and the bulk water in their idealized biofilm model that has later been widely accepted. As a result, oxygen flux into biofilms was generally calculated from observed oxygen gradients in the DO profiles by using Fick's diffusion laws, thereby obviating the need for indirect estimation of this flux. This method has been adopted ever since in biofilm research to interpret the phenomenon of oxygen transfer.

There are some assumptions behind this model. The first assumption is that there is a distinguishable biofilm surface. The second is that the DO profile in the diffusion layer above the water/biofilm interface is linear. The third is that the structure of biofilm is homogeneous, namely, density and microorganism distribution is uniform inside the biofilm, hence constant oxygen diffusivity is applicable to the entire biofilm (Lewandowski *et al.*, 1990).

However, many later studies, with applications of advanced research tools such as confocal scanning laser microscopy and microsensors, have proven that some of the above assumptions are not correct. Biofilm actually is much more heterogeneous than was believed and does not grow as a continuum rather as discrete microcolonies separated by sizeable pores or channels (Bishop, 1997; de Beer and Schramm, 1999). The biofilm structure changes with changes of water flow, especially the density at the surface and the distance of the filaments into the bulk water (Kugaprasatham *et al.*,

1992). Oxygen penetration into the biofilm varies with the physical structure of the biofilm and oxygen diffusivity in the biofilm varies with depth (Fu, 1993; Fu *et al.*, 1994; Zhang, 1994). Biofilm effective diffusivity (D_e) varies from 90 % of the diffusivity of oxygen in water (D_w) at the biofilm-liquid interface to about 25 % of D_w at the substratum of the biofilm. Yu and Bishop (1998) demonstrated the phenomenon of stratification of microbial processes in wastewater biofilms (Bishop and Yu, 1999). This stratification phenomenon can be attributed to the stratification of types of microorganisms (or ‘the allocation of bacteria species’ (Zhang and Bishop, 1994a) in biofilm that leads to the heterogeneity of biofilm structure.

The assumption of the DO profile in the diffusion layer being linear is only valid for stagnant water where molecular diffusion dominates oxygen transfer. In flowing water, convection exceeds diffusion, hence, a non-linearity of DO profile exists in the diffusion layer above the water-biofilm interface, and furthermore the thickness of this boundary layer is variable with external conditions such as bulk flow velocity (Lewandowski, *et al.*, 1993; Horn and Hempel, 1998).

Studies have shown that many factors influence oxygen transfer in wastewater biofilms and that usually only a thin layer of wastewater biofilms can be penetrated by dissolved oxygen. Chen and Bungay (1981) studied the influences of temperature, bulk water pH, age of biofilms, location within biofilms and microorganism concentration on oxygen transfer in wastewater biofilms taken from trickling filters. It was also reported that the bulk liquid DO concentration, the organic loading rate, the types of organics present, the presence of toxicants and the physical structure of the wastewater biofilm have significant influences on oxygen transfer in wastewater

biofilms (Fu, 1993; Fu and Bishop, 1993; Fu *et al.*, 1994; Zhang, 1994; Zhang and Bishop, 1994b, c; Zhang *et al.*, 1994, 1995). A catalog of the effects of these variables is very useful in designing a biofilm system for wastewater treatment and developing a flexible operating plan to maintain the system at its optimal conditions.

Modeling of biofilm processes is of great interest for reactor design and operation in wastewater treatment. Oxygen transfer in wastewater biofilms is one of the important aspects to be considered in modeling wastewater biofilm systems. As a result, the DO profiles measured directly from wastewater biofilms can play an important role in wastewater biofilm modeling.

Watanabe *et al.* (1982) proposed a biofilm model for system. This model was later verified by Nishidome and co-workers (1994) who conducted an *in-situ* DO measurement in a small scale RBC reactor in their laboratory. Based on their directly measured DO profiles, thickness of the attached-water film (L_w) at the air phase, the diffusion layer (L_d) at the water phase and oxygen flux to the wastewater biofilm were estimated and used for model verification.

Lewandowski *et al.* (1991) proposed a biofilm model that does not require that bulk oxygen concentration be known. The bulk oxygen concentration and bulk hydraulic conditions influence the biofilm respiration rate only through the shape of the DO profile. All parameters of the model are experimentally accessible. Based on the theoretical models and the DO profile, for their particular biofilm, the diffusion coefficient for DO ($D_f = 1.76 \times 10^{-5} \text{ cm}^2/\text{s}$), the oxygen flux through the biofilm surface ($J_{O_2} = 1.02 \times 10^{-6} \text{ mg/s} \cdot \text{cm}^2$) had been estimated.

Above progresses have provided us with better understandings of the nature of

oxygen transfer in biofilms. All these understandings are essential for rational optimization of biofilm reactor design and operation. However, in previous studies, the biofilm samples were either sampled directly from nature (e.g. stream) or biological wastewater treatment systems (e.g. RBC or trickling filter), or cultivated in small-scale model reactors in laboratory using artificial media or raw water collected from wastewater treatment systems. In other words, most of previous research work on wastewater biofilms has been done under artificial laboratory conditions. As a result, our current understanding of DO transfer in wastewater biofilms, in essence, is mainly based upon laboratory work. One major reason for this situation is the lack of suitable tools for direct DO measurement in wastewater biofilms in the field.

Laboratory study is usually the first step in research. The results obtained from the laboratory in many cases may be different from that from the real field conditions. With the results from the laboratory studies, our understanding of the nature of DO transfer in wastewater biofilms has been greatly advanced. However, can the conclusions be applied to wastewater biofilm systems in the real world? Can these existing models for oxygen transfer in wastewater biofilms, originally based on laboratory data, still correctly describe and predict the real situations under field conditions so as to help us optimize the design and operation of the wastewater biofilm systems? Answers to these questions have to be obtained through direct field studies.

This field study had two objectives. The first objective was to explore the feasibility of conducting *in-situ* DO measurement in wastewater biofilms in the field rather than in the laboratory. The second objective was to collect experimental

evidence under field conditions to verify the conclusions on DO penetration in wastewater biofilms previously made on the basis of laboratory studies.

Considering the availability and popularity of RBC system among biofilm systems employed in wastewater treatment, two domestic wastewater treatment plants using RBC systems were selected in the Province of Alberta, Canada, for this project. The DO concentration profiles in wastewater biofilms were measured directly on the RBC discs in the field. On the basis of these directly obtained *in-situ* data, DO penetration depth and oxygen flux in domestic wastewater biofilms were studied.

3.2 Site selection for field study

The field measurements in this study were conducted in two small towns (Devon and Olds) in the Province of Alberta. The town of Devon is located about 30 km southwest of Edmonton with an altitude of about 731 m. The current population in Devon is about 5,000. The town of Olds is located 220 km south of Edmonton with an altitude of 1,024 m. The population in the town of Olds is around 6,200. The domestic wastewater in both towns is treated by a wastewater treatment plant including primary and secondary clarifiers, and a RBC system in the between. The only difference in the RBC system between these two plants is the number of RBC stages. The RBC system in Devon has four stages, while in Olds it has six stages. In order to make comparisons between these two plants, the biofilm DO measurements were conducted only at the first four stages at both sites. General structure of the RBC system is illustrated in Figure 3.1. The major characteristics of the RBC systems and

wastewater qualities in these RBC systems at both sites are summarized in Table 3.1 and Table 3.2, respectively.

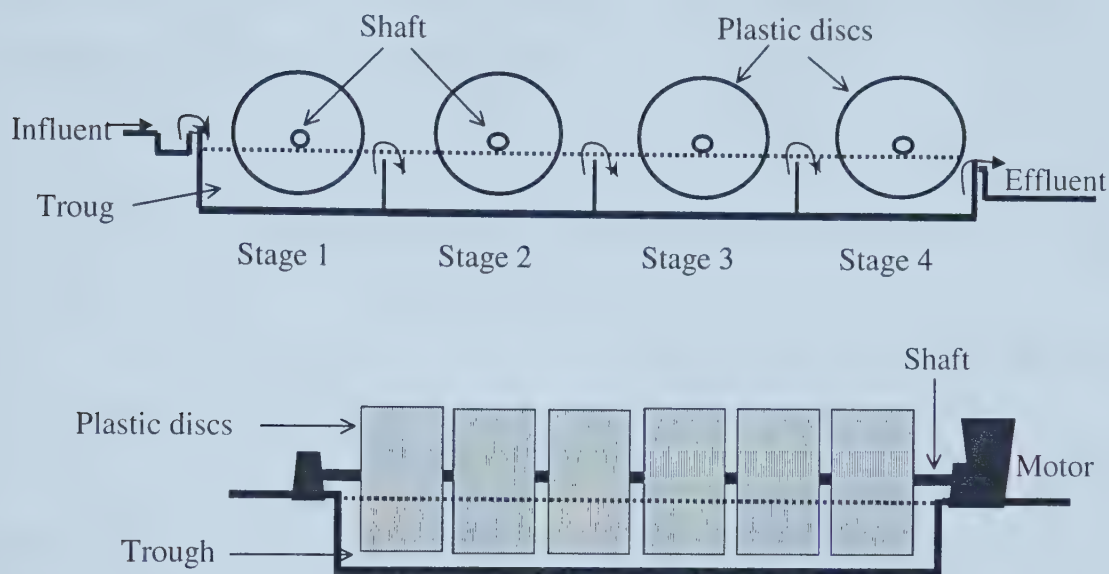


Figure 3.1. Schematic diagram of the RBC system. (Above: cross section of a four-stage RBC system; Below: cross section of one stage)

The influent to both wastewater treatment plants is domestic wastewater. Before it flows into the RBC system, the wastewater at both sites is treated by the primary clarifier. The major characteristics of the RBC systems at both sites are similar. They are also similar to those of typical RBC system designs (Grady *et al.*, 1999). These characteristics include disc diameter, disc effective area, disc submersion ratio, disc rotational speed, width of the trough, disc material, and effective trough volume. Furthermore, based on our examination of a number of RBC

systems, we concluded that these two selected sites are typical RBC systems and are good representatives for the RBC systems treating domestic wastewater. Consequently, biofilms growing on these two RBC systems are also good representatives for domestic wastewater biofilms. This makes the results from this field study more applicable to biofilm modeling.

Table 3.1 Major characteristics of RBC systems at Devon and Olds

Item	Stage							
	1		2		3		4	
	Devon	Olds	Devon	Olds	Devon	Olds	Devon	Olds
Rotational speed (r/min)	1.7	1.6	1.7	1.6	1.5	1.6	1.5	1.6
Disc diameter (m)	3.7	3.6	3.7	3.6	3.7	3.6	3.7	3.6
Disc thickness (mm)	1	1	1	1	1	1	1	1
Distance between discs (cm)	3	3	3	3	3	3	3	3
Disc material	HDPE*	HDPE	HDPE	HDPE	HDPE	HDPE	HDPE	HDPE
Width of the trough (m)	4.3	4.2	4.3	4.2	4.3	4.2	4.3	4.2
Length of the trough (m)	7.9	8.0	7.9	8.0	7.9	8.0	7.9	8.0
Water depth in tank (m)	1.5	1.5	1.5	1.5	1.5	1.5	1.5	1.5
Disc submergence depth (m)	1.4	1.4	1.4	1.4	1.4	1.4	1.4	1.4
Disc submersion ratio	40%	39%	40%	39%	40%	39%	40%	39%
Distance between water level and disc center (cm)	38.1	39.5	38.1	39.5	38.1	39.5	38.1	39.5
Disc effective area (m ²)	9290	9290	9290	9290	9290	9290	9290	9290
Effective tank volume (m ³)	50.9	50.4	50.9	50.4	50.9	50.4	50.9	50.4
Water flow rate (L/sec)	8-80	25-65	8-80	25-65	8-80	25-65	8-80	25-65
Influent retention time (min)	11-106	13-33	11-106	14-36	11-106	13-33	11-106	13-33
Start-up time of operation	08/'95	09/'97	08/'95	05/'00	08/'00	09/'97	06/'80	03/'00

* High density polyethylene.

Table 3.2 Water quality in RBC systems at Devon and Olds*

Stage	Parameter	Devon	Olds
Influent	TSS (mg/L)	125	63
	BOD (mg/L)	109	184
	pH	7.8	7.5
	Temperature (°C)	15.5	15.3
	DO (mg/L)	3.3	<1.0
Stage 1	TSS (mg/L)	89.5	63
	BOD (mg/L)	55.6	80.8
	pH	7.6	7.4
	Temperature (°C)	14.8	12.1
	DO (mg/L)	2.0	1.6
Stage 2	TSS (mg/L)	91.5	80
	BOD (mg/L)	42.6	30.7
	pH	7.7	7.5
	Temperature (°C)	15.0	12.1
	DO (mg/L)	1.4	3.9
Stage 3	TSS (mg/L)	79.5	105
	BOD (mg/L)	24.9	20.5
	pH	7.6	7.5
	Temperature (°C)	15.0	12.3
	DO (mg/L)	1.8	4.1
Stage 4	TSS (mg/L)	69	107
	BOD (mg/L)	28	13.3
	pH	7.6	7.5
	Temperature (°C)	14.8	12.3
	DO (mg/L)	3.9	5.0

* Adapted from plants measured during May, 2001 in Devon and June, 2001 in Olds when the studies were conducted at respective sites.

3.3 Materials and methods

The most important research tool for the field DO measurements in wastewater biofilms was the oxygen microelectrode. After the oxygen microelectrode was fabricated in our laboratory, an evaluation of it was conducted before it was taken out of the laboratory for the field measurements. The oxygen microelectrode used in this field study had a tiny tip with a diameter around 15 μm . Due to its fragility, the oxygen microelectrode had to be mounted on a very solid and stable platform to prevent it from being broken during the measuring processes. In addition, the conditions at each RBC system might be somewhat different. For example, the distance from the trough edge to the disc, the local space available for experimental setup, the configuration of the RBC discs, and the supporting frame of the discs might all be different. Therefore, the platform had to be designed with flexibility to suit different site conditions.

Based upon the results of our preliminary field investigation, a special setup shown in Figure 3.2, was designed to satisfy the special needs for direct biofilm DO measurement in the field. This entire setup is made of steel with a heavy base that guarantees a solid platform without significant vibration. The setup can be conveniently dismantled for transportation from one place to another during the fieldwork. The square base comprises two steel plates, one stacked on top of the other, fixed together with four screws. There are another four tapped screws, one for each corner of the base, which can be used for leveling the whole setup on uneven ground. The vertical steel column can be mounted and fastened on the base through

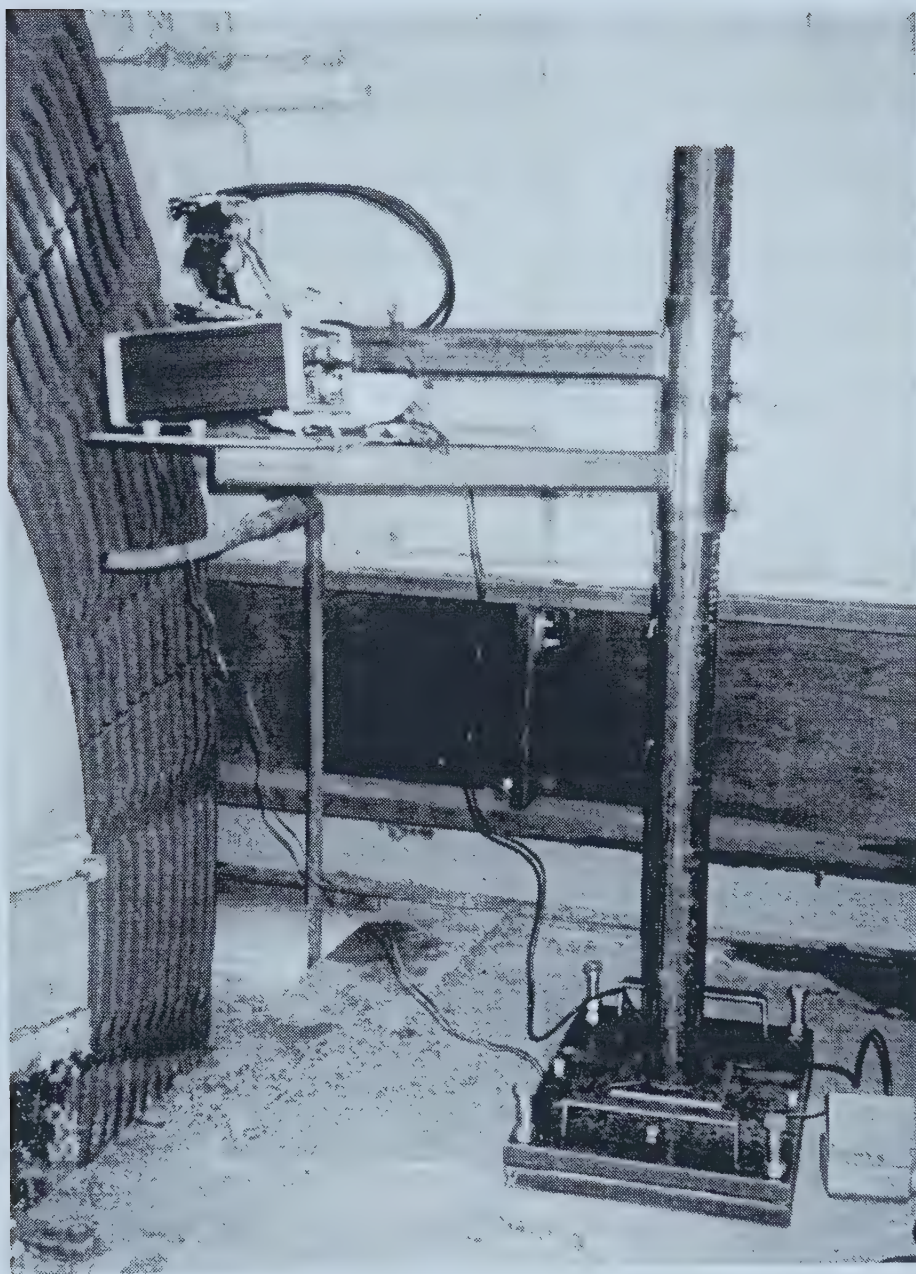


Figure 3.2 Setup for DO measurement in RBC biofilms using an oxygen microelectrode

four screws. There are three vertically adjustable arms, each with a plate at the front part of the arm. The three arms are for the installation of the micromanipulator, the picoammeter and the light source. Furthermore, the arm for the micromanipulator comprises two parts with one having an outer diameter equal to the inner diameter of the other so as to obtain a perfect engagement with each other. This configuration makes the arm horizontally adjustable to facilitate the movement of the oxygen microelectrode toward the biofilms on the RBC discs during direct biofilm DO measurements in the field.

Normally, the field environment of the RBC systems is not bright enough for the extremely delicate work of direct DO measurement in biofilms. Fortunately, unlike natural biofilms, the majority of microorganisms in biofilms in biological wastewater treatment systems are non-photosynthetic rather than photosynthetic (Kuenen *et al.*, 1986). In order to provide a light spot on the biofilm surface that is adequately bright to facilitate the DO measurements with fragile oxygen microelectrode, a light source (Schott Glas, Weisbaden, Germany; Model KL1500 LCD) was used. This light source can provide a special light that is bright enough for the work but does not generate significant temperature change on the surface of the biofilms. This characteristic is particularly important for DO measurement in the biofilm, because significant temperature change would affect the biofilm and DO in it.

In the field, this setup was placed on the edge of the trough at one end of the RBC shaft. Suitable heights were selected for all three arms so as to make sure the following conditions were met: (1) The selected spot of biofilm on the RBC disc could be reached by the oxygen microelectrode; (2) the distance between the oxygen

microelectrode and the picoammeter was within the length of the connection cables; (3) a suitable distance (normally about 30 cm) between the light source and the biofilm spot to be measured could be obtained without significantly weakening the brightness of the light and causing temperature change on the biofilm surface; (4) the signal readings on the picoammeter could be seen and recorded conveniently; and (5) the micromanipulator could be operated as conveniently as possible.

Before the DO measurement in the biofilm at a certain stage was conducted, polarization and calibration of the oxygen microelectrode was carried out again. In order to obtain accurate results, the wastewater used for each polarization and calibration process was sampled from the corresponding stage. During the calibration process, the tip of the oxygen microelectrode could have been broken by some coarse suspended solids in the wastewater that would have been quickly stirred up during the gas flushing. In order to prevent this from happening, the sampled wastewater was first filtered through a coarse qualitative filter paper (Whatman, Clifton, NJ, USA; Cat. No. 1002185) before being used for the calibration.

Once the calibration was finished, the oxygen microelectrode was mounted onto the micromanipulator that had been installed in advance on the setup. During this process, the oxygen microelectrode was usually kept connected to the picoammeter so as to avoid another long waiting period to obtain a stable reading of the oxygen microelectrode. Since the oxygen microelectrode was not installed onto the RBC disc hence rotating with the disc, the motor driving the RBC discs had to be turned off and the RBC discs had to be completely stopped just before the DO measurement in the biofilm started. Nishidome *et al.* (1994) reported that the DO profiles of RBC biofilm

alternately rotating between the air and the water phases reached steady state only within several seconds in both phases. This means that in our case keeping RBC discs stopped and exposed to the air phase has no significant impact on DO profiles in RBC biofilms. In other words, the status of DO profiles in a stopped RBC biofilm is similar to those in a rotating RBC biofilm after it has been exposed to the air for several seconds, because in both cases, the DO profiles in wastewater biofilms are all at steady status.

During DO measurement in the biofilm, the oxygen microelectrode was first moved toward the biofilm and then stopped at about 0.5 – 1.0 mm above the biofilm surface. After that point, the oxygen microelectrode was further moved toward the biofilm substratum with a fixed interval of depth (50 or 30 μm). Meanwhile, the readouts of the current signal on the picoammeter were recorded for each interval. Considering the response time of the oxygen microelectrode was less than 2 seconds, in the data recording process, a readout was accepted when about 2 seconds had passed after the oxygen microelectrode was advanced with one fixed interval of depth toward the biofilm substratum. This movement of oxygen microelectrode toward the biofilm substratum and the readout recording process were continued until at least three consecutive zero readouts were recorded.

At the first and second RBC stages at Devon, there is a metal frame fixing the RBC discs and rotating with these RBC discs. As a result, there are also biofilms growing on the surface of these metal frames. In order to make comparisons between metal substratum and plastic substratum, DO penetration into biofilms growing on the surface of metal frames were measured as well as those on the plastic substratum (i.e.

RBC disc).

In this study, the principle for DO measurement in the field was that at each stage at least two DO profiles should be measured. However, due to the complicated and sometimes unpredictable conditions in the fields, this principle could not always be followed. As a result, when the field conditions were good, more DO profiles at one stage were measured; when field conditions did not permit, fewer measurements were done.

After the DO measurement, a Pasteur pipette with a capillary end was mounted onto the same micromanipulator to replace the oxygen microelectrode. This special Pasteur pipette was made in the same way as the outer casing of the oxygen microelectrode was made, but this special pipette had a bigger open tip which is conducive to observation of water suction in it. After being mounted, this capillary was advanced toward to the biofilm. Once water suction was observed within the capillary, this means that the capillary touched the biofilm surface and the reading on the scale of the micromanipulator was recorded as the initial value. Afterwards, the capillary was further moved toward the biofilm substratum and finally touched the substratum, the capillary would break, which could be detected either by a cracking sound and/or by increased resistance in advancing the micromanipulator. The reading on the scale of the micromanipulator was recorded as the ultimate value. The difference between these two recorded values was interpreted as the thickness of the biofilm.

3.4 Results and discussions

During DO measurement, the oxygen microelectrode was advanced gradually from the air phase above the wastewater biofilm into the wastewater biofilm. However, the research subject in this field study was actually the DO within the wastewater biofilm, rather than the oxygen in the air. Therefore, the surface of the wastewater biofilm had to be determined first. Only based upon the determined reference point, the biofilm surface, can other associated issues such as the DO penetration depth within the wastewater biofilm and the oxygen flux into the wastewater biofilm be determined. As a result, in the following sections, the determination of the biofilm surface is first discussed.

3.4.1 Determination of biofilm surface

Several studies have reported that a liquid layer between the air and the biofilm exists when RBC biofilm is exposed to the air phase and that a diffusion layer exists between the bulk liquid and the biofilm when the biofilm is submerged in the water phase (Sanders *et al.*, 1971; Williamson and McCarty, 1976; Watanabe *et al.*, 1980; Nishidome *et al.*, 1994). However, there has not been a method that can accurately estimate the thickness of these layers. It is widely accepted that the thickness of these layers is dependent on the configuration of biofilm surface and the flow velocity of the bulk liquid or the rotational speed of the RBC disc.

Bintanja *et al.* (1975) and Zeevalkink *et al.* (1978) studied the relationship between the thickness of the attached water film on the rotating disc and the rotational

speed of the disc. Both studies concluded a linear relationship between the thickness of the attached water film and the square root of the rotational speed of the disc, although their expressing equations are slightly different. Bintanja *et al.* (1975) concluded the linear equation with a form of

$$\delta = \kappa (\eta \omega Y / \rho g)^{1/2} \quad (3.1)$$

where, δ = thickness of the attached water film; $\kappa = 0.93$; η = dynamic viscosity of the water; ω = rotation speed of the disc; Y = radius of the disc; ρ = density of the water; and g = gravitational acceleration constant.

while Zeevalkink *et al.* (1978) used an equation of

$$\delta = 4/15 (2 \nu \omega / g)^{1/2} (R^2 - H^2)^{1/4} \quad (3.2)$$

where, δ = thickness of the attached water film; ν = kinematic viscosity of water; ω = rotation speed of the disc; g = gravitational acceleration constant; R = radius of the disc; and H = distance between water level and shaft.

Although they conducted their tests only under relatively high rotational speeds (6 to 35 rpm), they interpolated their results for lower rotational speeds down to zero, which led to a thickness of zero of the attached water film. This is clearly illustrated in Figure 3.3.

Based on this relationship, Watanabe *et al.* (1982) estimated a thickness of 40 μm of the attached water film on RBC disc at a rotational speed of 7.5 rpm using

equation (3.1). Spengel and Dzombak (1992) reported a thickness of 20 μm of the attached water film at a rotational speed of 2.3 rpm using equation (3.2).

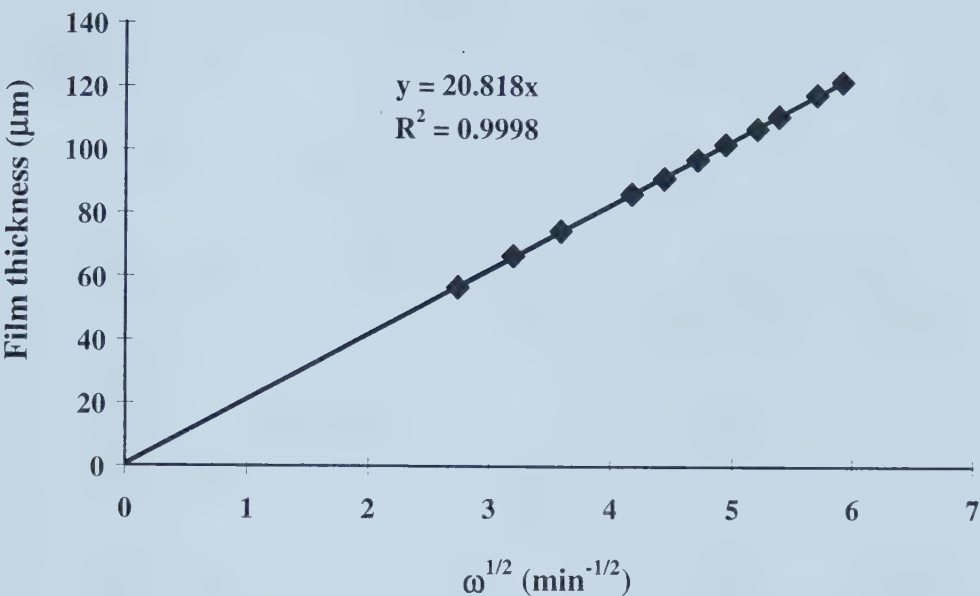


Figure 3.3 Thickness of attached water film on RBC disc as a function of $\omega^{1/2}$ (Modified from Bintanja *et al.*, 1975)

In this study, the rotational speed was zero because the disc was stopped before the DO measurement. Therefore, the thickness of the attached water film would be zero according to the above relationship. However, due to uneven and sponge-like nature of the biofilm surface, there was actually still water existing at the biofilm surface even though the RBC disc stopped. This kind of water may be considered as one of the inseparable and indispensable components of the biofilm itself rather than an attached water film outside of the biofilm. In other words, biofilms on the RBC disc in this study were under the most favorable condition in terms of oxygen

availability to microorganisms in the biofilm. This is because in this case oxygen transfers directly from the air to the biofilm without the barrier of an attached water film over the biofilm. Figure 3.4 shows how the biofilm surface is determined in this study based upon the above linear relationship. The original data for Figure 3.4 are listed in Appendix 3.1.

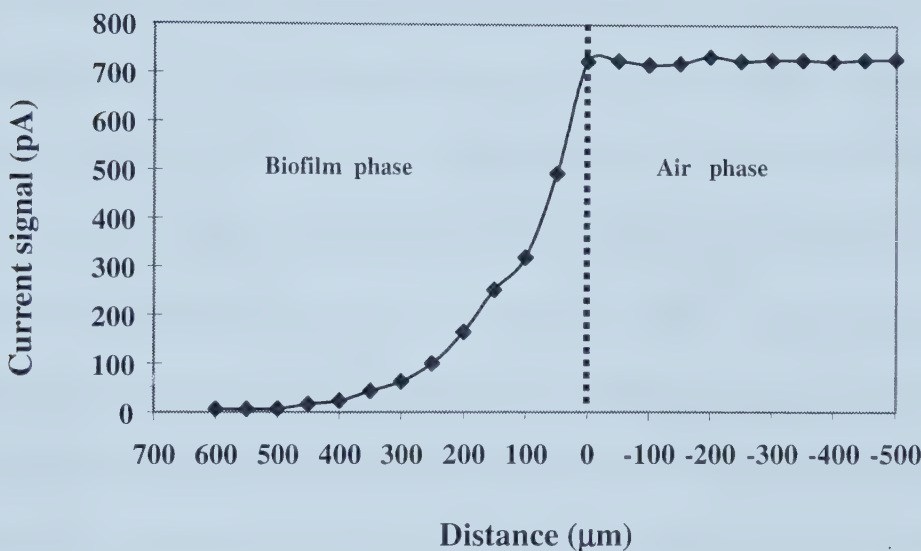


Figure 3.4 Determination of the biofilm surface

In Figure 3.4, the DO profile can be separated into two parts. The first part is the leveled curve that comprises those readings when the oxygen microelectrode was above the RBC biofilm and in the air phase. The second part is a sharply decreasing curve that comprises all those readings when the oxygen microelectrode was moved down into the biofilm. As discussed early, in our case, there was no attached water

film over the surface of biofilm. As a result, the inflection point on the DO profile can be determined as the point where the biofilm surface is.

3.4.2 DO profiles in wastewater biofilms

After the biofilm surface was determined, the DO profiles within biofilms can then be constructed. The constructed DO profiles within wastewater biofilms at all the first four stages of the RBC systems at both Olds and Devon are illustrated in Figure 3.5 through Figure 3.12. The original data for all these figures are listed in Appendix 3.2. In these figures, "0" on the x-axis stands for the place of the biofilm surface.

At Devon, biofilms growing on the 3rd stage was found the thinnest after we compared biofilm thickness between all those four RBC stages before all DO measurements got started. Therefore, in order to prevent the oxygen microelectrode from being broken during the measurement, DO measurements in biofilms at the 3rd stage had not been made until DO measurements at other three stages were completed. During the DO measurement at the 3rd stage, a very erratic reading showed up after the oxygen microelectrode had been moved toward the substratum for a certain distance. Further measurement was stopped immediately at this point and this oxygen microelectrode was checked under the microscope. As expected, the tip of this oxygen microelectrode had been broken. As a result, only one DO profile was determined at the 3rd stage at Devon. Based upon this phenomenon, the thickness of biofilm at this specific measurement spot finally was determined as around 0.75 mm directly from the DO profile shown in Figure 3.11.

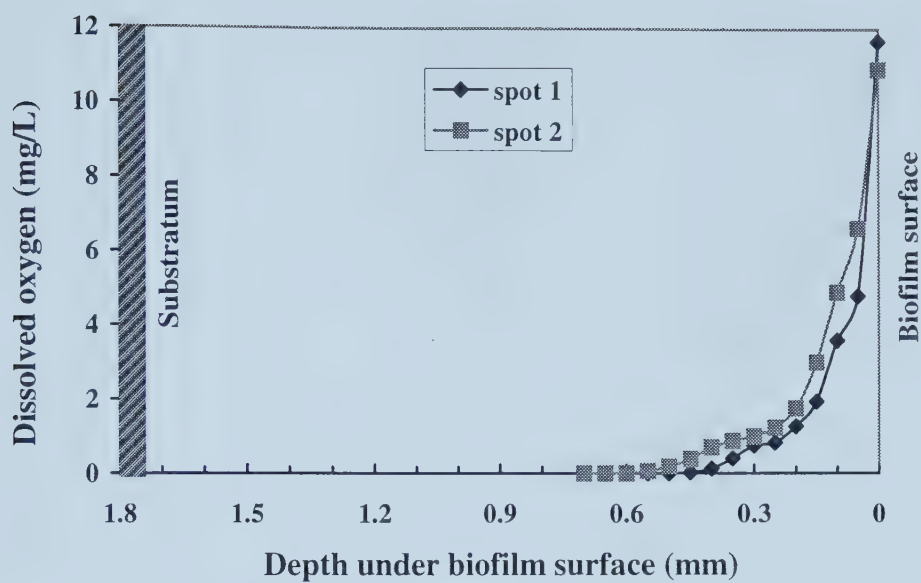


Figure 3.5 DO profiles in biofilms at Stage 1 at Olds

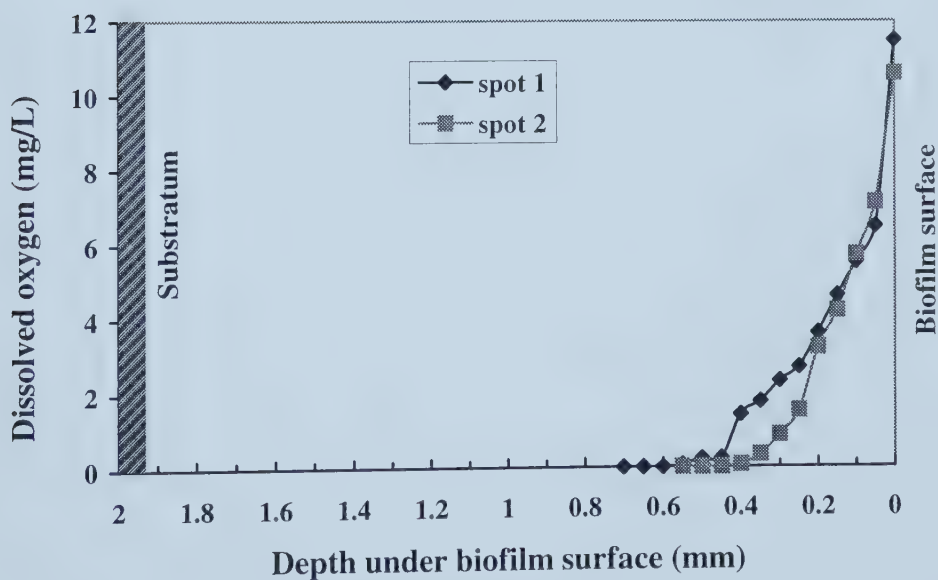


Figure 3.6 DO profiles in biofilms at Stage 2 at Olds

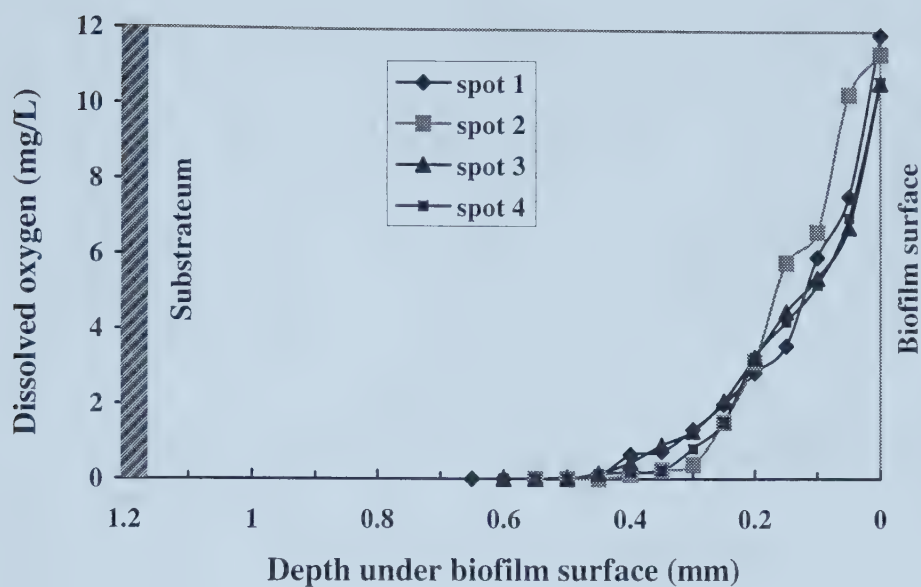


Figure 3.7 DO profiles in biofilms at Stage 3 at Olds

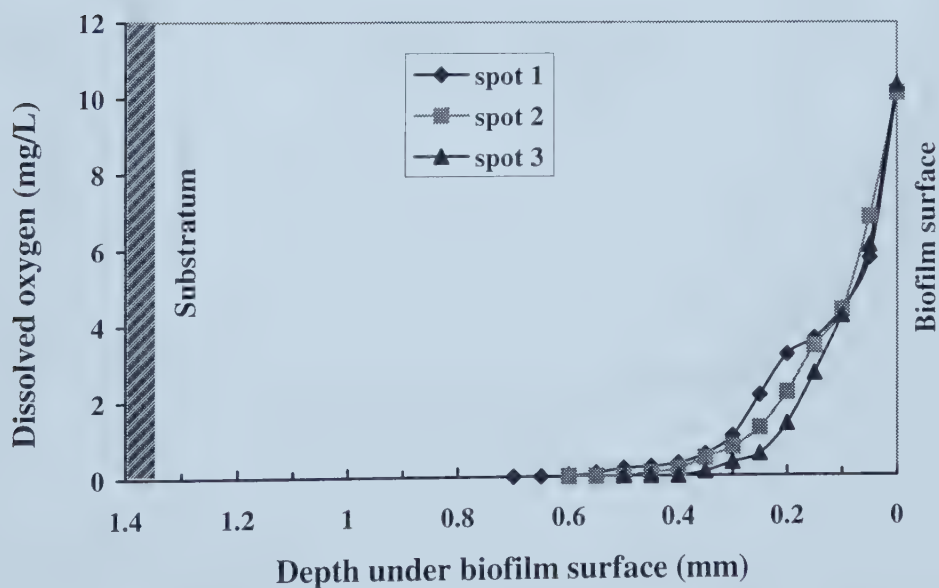


Figure 3.8 DO profiles in biofilms at Stage 4 at Olds

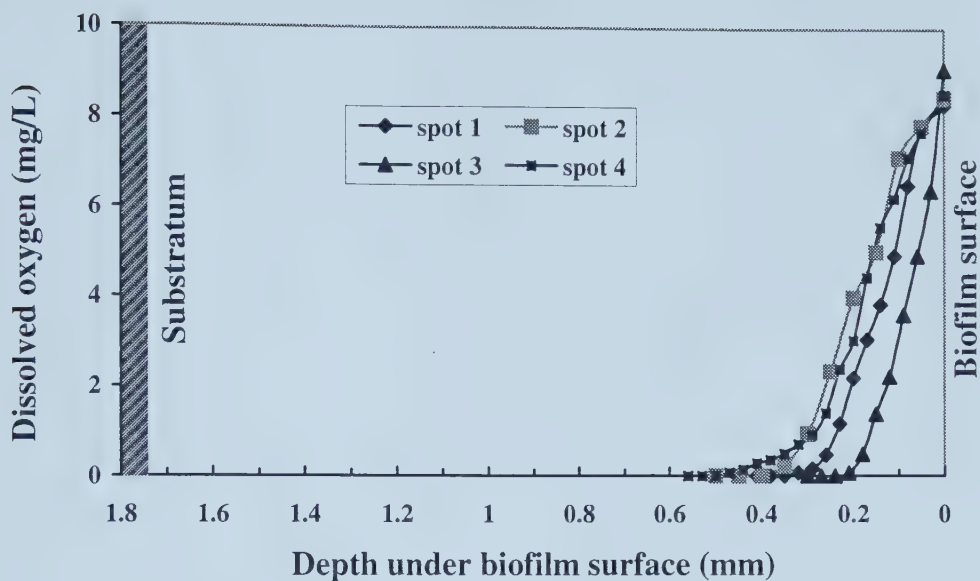


Figure 3.9 DO profiles in biofilms at Stage 1 at Devon

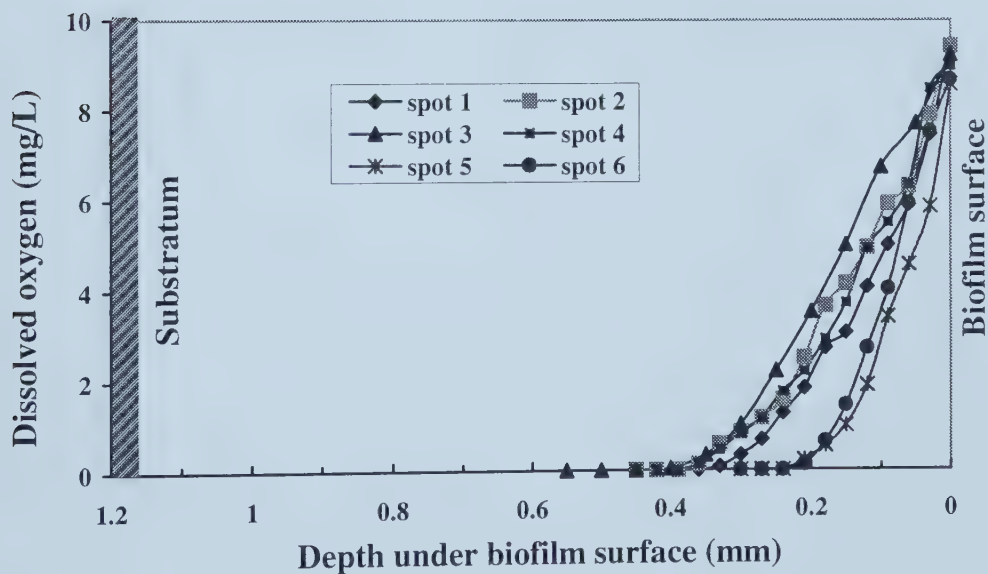


Figure 3.10 DO profiles in biofilms at Stage 2 at Devon

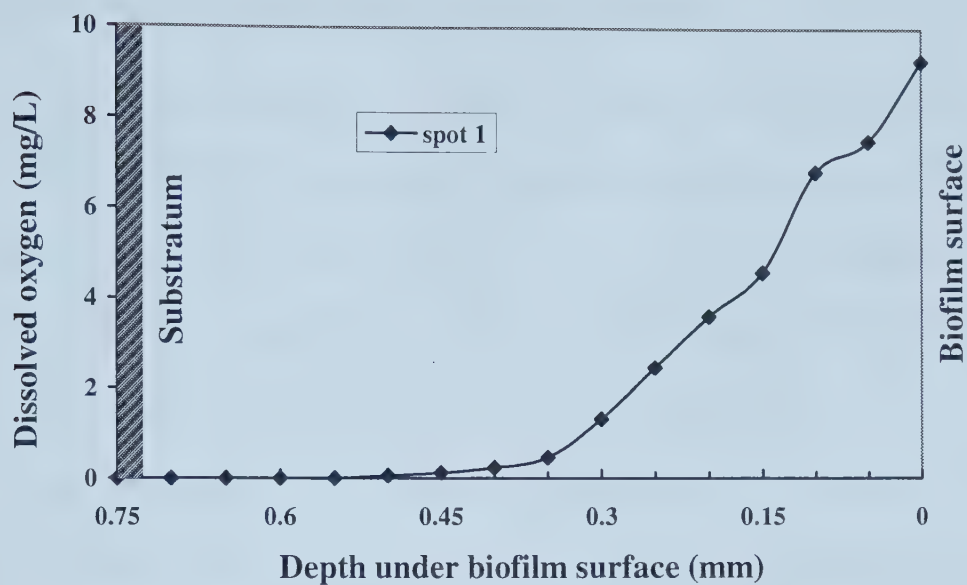


Figure 3.11 DO profile in biofilms at Stage 3 at Devon

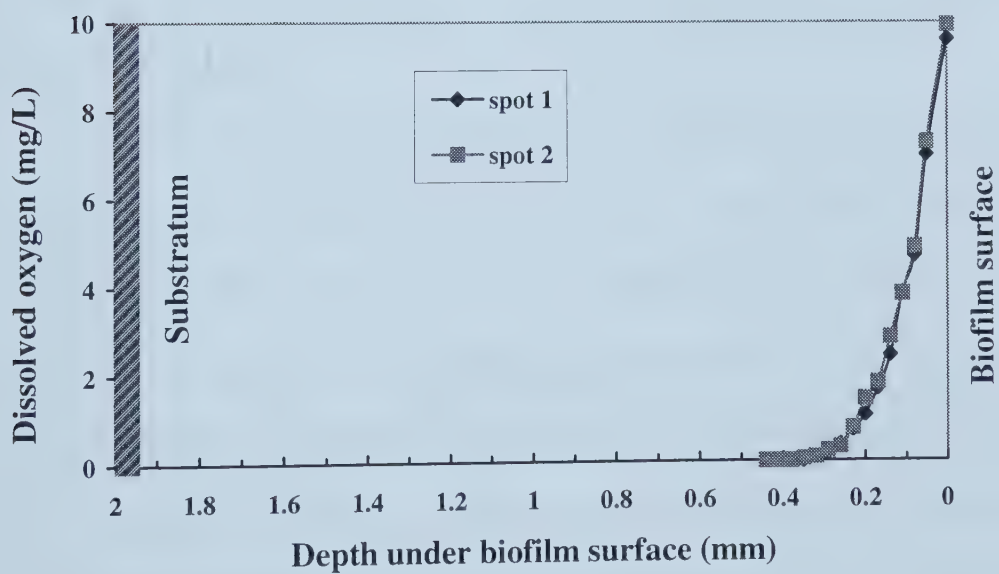


Figure 3.12 DO profiles in biofilms at Stage 4 at Devon

3.4.3 Oxygen penetration depth in wastewater biofilms

As an important index, the depth of oxygen penetration can help reveal the chemical conditions, bacteria distributions and microorganism activities in wastewater biofilms. After the construction of the DO profile, the oxygen penetration depth in biofilm can now be determined. Results of the determination of DO penetration depth in wastewater biofilms at Devon and Olds are summarized in Table 3.3.

As mentioned in the “Materials and methods,” the numbers of the DO measurements at each stage varied depending upon the field conditions at the time when the DO measurements at a specific stage were conducted. As a result, more DO measurements were conducted at some stages than others as can be seen in Figure 3.5 to Figure 3.12. This is also reflected by DO penetration depth determinations summarized in Table 3.3.

From all those DO profiles (Figure 3.5 to Figure 3.12), it has been seen that compared with the thickness of wastewater biofilm, DO penetration depth was only a fraction of the biofilm thickness. There was no one biofilm at any stage of both RBC systems at Olds and Devon that was fully penetrated by DO. In Table 3.3, it has been learnt that DO penetration depth in wastewater water biofilms ranged from 240 μm to 600 μm . These findings were made under the most favorable condition with respect to oxygen penetration into the biofilms for the RBC systems. That is, during the DO measurement the RBC discs were stopped and exposed to the air phase instead of being rotated in the water and air phases alternately during the measurement. This condition allowed the maximum possible oxygen penetration into the biofilms on the

Table 3.3 DO penetration depths in biofilms at Devon and Olds

Unit: μm

Stage	Measurement spot	Devon	Olds
1	#1	350	500
	#2	400	600
	#3	240	-
	#4	500	-
2	#1	360	600
	#2	390	450
	#3	450	-
	#4	390	-
	#5	240	-
	#6	240	-
3	#1	550 *	550
	#2	-	450
	#3	-	500
	#4	-	500
4	#1	350	600
	#2	380	500
	#3	-	400

* After this measurement, the oxygen microelectrode was broken. As a result, only one measurement was obtained for the 3rd stage at Devon.

RBC discs under the field conditions. As a result of the partial oxygen penetration in biofilms, a biofilm can be divided along its depth into aerobic and anoxic zones in terms of oxygen existence within biofilms. It can be further deduced that the major aerobic microbial processes such as carbon oxidation and nitrification can only take place within this thin aerobic layer where oxygen is available. This could significantly

affect the effectiveness of the biofilm systems and the efficiency of substrate removal in the systems.

A number of previous studies have reported that oxygen penetrates only into the top portion of the biofilms (Lewandowski *et al.*, 1990; Zhang, 1994; Yu, 2000, Li and Bishop, 2000). These reports of partial oxygen penetration in biofilms were based upon laboratory investigations. What is the situation in wastewater biofilms under field conditions? There has not been direct measurement of wastewater biofilms under field conditions to confirm the findings made in laboratories. The experimental results obtained under field conditions in this study have provided for the first time the direct experimental evidence to answer the above question. These experimental results not only support the laboratory findings but also demonstrate that oxygen can not fully penetrate the wastewater biofilms even under the most favorable condition (oxygen transfers directly into the wastewater biofilms from the air phase without the barrier of the attached water film).

It has also been revealed from those DO profiles (Figure 3.5 to Figure 3.12) that the phenomenon of partial oxygen penetration in wastewater biofilms occurred at every stage of the RBC system at both wastewater treatment plants. Since these plants are good representatives of domestic wastewater biofilms, the findings from this study could be applied in general to wastewater biofilms. Therefore, it can be concluded that partial oxygen penetration is a common phenomenon in wastewater biofilms under field conditions. This conclusion should be helpful for biofilm system design and operation for domestic wastewater treatment.

3.4.4 Comparison of DO penetration depth between different RBC stages

In order to compare oxygen penetration depth in biofilms at different RBC stages, the DO profiles were constructed for all four stages at Devon and the first four stages at Olds. The average values (with standard deviation) of the measured oxygen penetration depths in biofilms at different RBC stages but with the same substratum materials – plastics - are summarized in Table 3.4.

Table 3.4 Comparison of DO penetration depth between different RBC stages

Stage	DO penetration depth (µm)			
	Olds		Devon	
	Average	SD*	Average	SD
1	550	± 71	375	± 35
2	525	± 106	375	± 21
3	500	± 41	550**	0**
4	500	± 100	365	± 21

* Standard Deviation;

** Only one measurement was made at this stage.

When comparing oxygen penetration depths between different RBC stages, it has been seen that there was not significant difference on oxygen penetration depth in both RBC systems. This was particularly true at Olds, where the average oxygen penetration depths between stages varied from 500 µm to 550 µm. The difference here was only 50 µm. However, the standard deviations in oxygen penetration depth

at most of these four stages were much larger. They varied from 71 μm at the first stage and 100 μm at the forth stage to 106 μm at the second stage, all of which were much bigger than the difference of average DO penetration depth (50 μm). This meant that the difference in oxygen penetration depth between different measurement spots at the same stage was bigger than that between different stages. Although the third stage seemed to be an exception, its standard deviation still reached 41 μm .

Excluding the third stage, which might be a special case and is discussed in detail later in this chapter, it still could be said that the similar phenomenon on oxygen penetration in biofilms between RBC stages was observed at Devon as well. Except for the third stage, the average oxygen penetration depth varied from 365 μm to 375 μm between stages. The difference was only 10 μm . In contrast, the standard deviations in oxygen penetration depth at all three stages were 35 μm for the first stage and 21 μm for both Stage 2 and 4.

As a result, possible influence, if any, brought in by the order of RBC stages, on DO penetration depth was not as significant as that brought in by the spot (location) of the DO measurement on the biofilms. Such a phenomenon is more clearly illustrated in Figure 3.13. This phenomenon may be attributed to the heterogeneous nature of the biofilm structure. It is this kind of structure heterogeneity of the biofilm that made its associated characteristics such as oxygen penetration depth often unevenly distributed over the entire wastewater biofilms on the RBC discs. In other words, the oxygen penetration depth in wastewater biofilms differs from spot to spot and the DO measurement in wastewater biofilms is site specific.

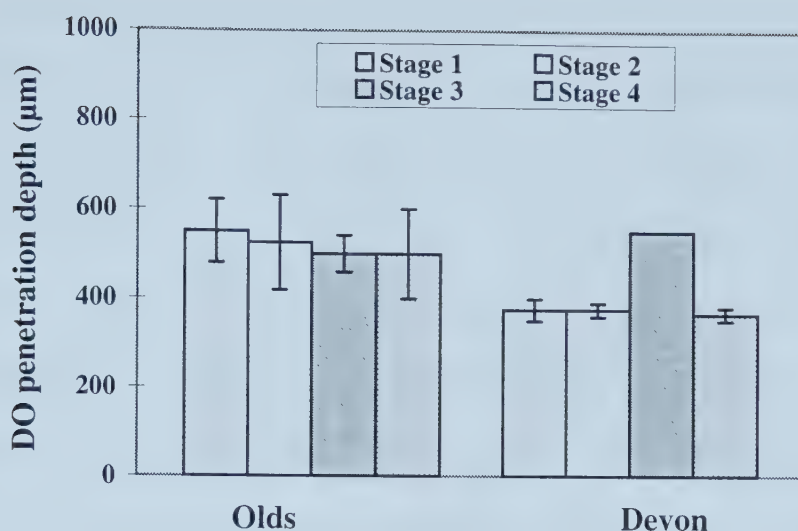


Figure 3.13 Comparison of DO penetration depth between different RBC stages
(Note: Only one DO profile measured at Stage 3 at Devon)

3.4.5 Comparison of DO penetration depth between different substrata

In the four stages of the RBC system at Devon, there are two stages using a configuration with metal frames that run with all those plastic discs. As a result, there is also biofilm growth on these metal frames. The DO measurements of these biofilms were carried out so that a comparison on the oxygen penetration in biofilms growing on different materials can be made. The comparison of oxygen penetration depths within wastewater biofilms growing on metal and plastic materials is illustrated in Table 3.5.

In Table 3.5, it has been seen that there was no big difference in DO penetration depth between biofilms growing on metal substratum and plastic substratum. At Stage 1, the average DO penetration depths for both types of

substratum materials were very close, 370 μm for the metal and 375 μm for the plastic. Their difference was only 5 μm . However, the standard deviations for the metal and plastic substrata were 184 μm and 35 μm , respectively. The similar phenomenon was observed at Stage 2. This is more clearly shown in Figure 3.14. Based on these observations, it can be concluded that the difference in oxygen penetration depth in wastewater biofilms brought in by different measurement spots is more significant than those brought in by different types of biofilm substratum materials. In other words, no clear impact that the type of substratum material brought in on oxygen penetration depth within wastewater biofilms could be concluded. Further studies on the impact of substratum material need to be conducted in laboratory where experimental conditions can be controlled so that more comparable data can be obtained for analysis

Table 3.5 Comparison of DO penetration depth between different substrata

Unit: μm

Stage	Metal substratum		Plastic substratum	
	Average	SD*	Average	SD
1	370	± 184	375	± 35
2	330	± 107	375	± 21

* Standard Deviation.

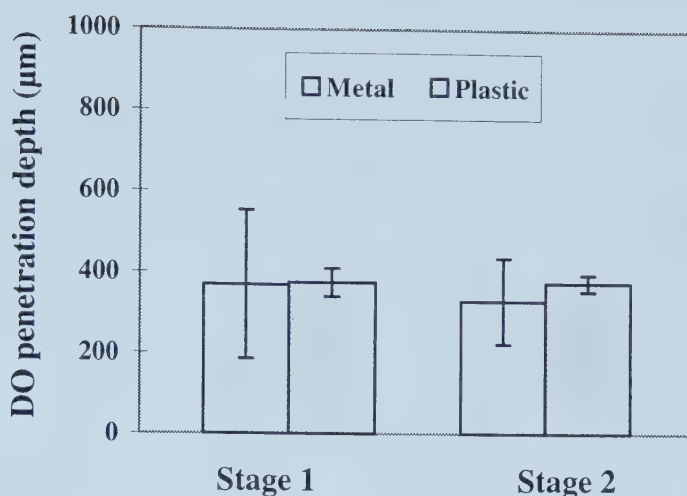


Figure 3.14 Comparison of DO penetration depth between different substrata

3.4.6 Comparison of DO penetration depth between different plants

A comparison of DO penetration depth in biofilms growing on the same substratum material (plastics) between two RBC systems at Devon and Olds is made in Table 3.6.

From the data in Table 3.6, it can be seen that oxygen generally penetrated deeper in biofilms at Olds than at Devon. At Olds the oxygen penetration depth had the range from 400 μm to 600 μm , while at Devon it had the range from 350 μm to 400 μm , except for the third stage in which the oxygen penetration depth reached 550 μm .

Table 3.6 Comparison of DO penetration depth between different plants

Unit: μm

Stage	Measurement spot	Devon	Olds
1	#1	350	500
	#2	400	600
2	#1	360	600
	#2	390	450
3	#1	550 *	550
	#2	-	450
	#3	-	500
	#4	-	500
4	#1	350	600
	#2	380	500
	#3	-	400

*After this measurement, the oxygen microelectrode was broken. As a result, only one measurement was obtained for the 3rd stage at Devon.

An interesting phenomenon here is that the oxygen penetration depth at the third stage at Devon was very close to those at Olds. This phenomenon led to the search for the possible reason behind it. The phenomenon indicated that the oxygen penetration depth in the third stage at Devon was close to those at Olds but different from those of the other stages at Devon. This inspired us to find the similarity between the third stage of Devon and the RBC stages at Olds and the difference between the third stage of Devon and the other stages of the same RBC system. After comparing the operational information of both RBC systems, we found that the start-up time for a particular stage could provide us with the possible explanation.

As listed in Table 3.7, the start-up times for these stages are as follows: at Devon, the fourth stage started in 1980, the first and second stages started in August 1995, and the third stage started recently in August 2000. At Olds, the first and third stages started in September 1997, the fourth stage started in March 2000, and the second stage started in early May 2000. All of the stages at Olds started their operation much later than the stages at Devon, except for the third stage of Devon.

Table 3.7 DO penetration depths and the start-up time of RBC stages

Stage	DO penetration depth * (μm)		Start-up time	
	Devon	Olds	Devon	Olds
1	375	550	08/1995	09/1997
2	375	525	08/1995	05/2000
3	550	500	08/2000	09/1997
4	365	500	06/1980	03/2000

* Average values calculated from Table 3.6 for each RBC stage at Devon and Olds.

Such a consistent relationship between the start-up time for a particular stage of a RBC system and the oxygen penetration depth in the biofilm on the RBC discs in that stage suggests a certain correlation between these two variables. For the RBC discs with a shorter operation time, the biofilm on it may have a relatively loose structure hence a relatively low density and uneven biofilm surface, which facilitate deeper oxygen penetration into the biofilms. In contrast, for the RBC discs with a

longer operation time, the biofilm on it may have a more compact structure and hence a high density, which hinders the oxygen penetration into the biofilms. Although biofilm sloughing occurs periodically during operation, there might still be a build-up effect for those biofilms on the RBC discs with long operation time.

Based on the experimental observations in this study and the above analysis, it can be concluded that the oxygen penetration depth for biofilms with shorter operation time is greater than that for biofilms with longer operation time. Although an ultimate explanation on this phenomenon needs to be made based on more studies in the future, this relationship itself, if correct, still can provide constructive suggestions to biofilm system design and operation. For instance, if good aerobic biofilms are desired in a RBC system, enforced sloughing measures could be designed to replace the natural sloughing process. This would promote the growth of biofilms with shorter operation time, hence increase the oxygen penetration depth in the biofilms.

3.4.7 Estimation of oxygen flux into wastewater biofilms

Oxygen flux is an important index for oxygen transfer study in biofilms. A number of laboratory studies have estimated the value for this index. The commonly used method in the estimation of the oxygen flux into biofilms is using Fick's diffusion law and adopting a constant value for oxygen diffusivity in biofilms. However, a number of recent biofilm studies (Bishop, 1997; de Beer and Schramm, 1999) have reported that the structure of biofilms is heterogeneous rather than homogeneous as used to be widely believed. Oxygen penetration into the biofilm varies with the

physical structure of the biofilm and oxygen diffusivity in the biofilm varies with depth (Fu, 1993; Fu *et al.*, 1994; Zhang, 1994). The results of this field study have also proven the conclusion that biofilms are structurally heterogeneous.

Despite these new discoveries, the assumption that biofilm is structurally homogeneous and hence the application of a constant oxygen diffusivity in biofilms is still a necessary simplification to estimate oxygen flux into biofilms by applying Fick's diffusion law. At least it's the case before a new practicable model in which these new discoveries are integrated has been developed. This simplified method has been employed by many researchers, and a lot of meaningful achievements in study on oxygen transfer in biofilms have been made (Chen and Bungay, 1981; Kuenen *et al.*, 1986; Nielsen *et al.*, 1990; Lewandowski *et al.*, 1991; Nishidome *et al.*, 1994; Cheng, 1996; Chen and Huang, 1996; Horn and Hempel, 1997).

Nishidome and Kasuda (1988) studied oxygen flux into biofilms in a small model RBC reactor in their laboratory when the RBC was at rest exposed to the air phase for 60 seconds. In a later laboratory study, Nishidome *et al.* (1994) estimated oxygen flux into biofilms when the RBC disc was exposed to the air phase for 30 seconds without stopping rotation. In both of these studies, above simplified assumption was accepted and a constant oxygen diffusivity was used for oxygen flux estimations. Using this method and their DO profiles constructed based on their laboratory data, they had verified an early RBC biofilm model.

Compared with their studies, this study has two significant aspects different. The first difference is that this study was conducted under field conditions rather than

in a laboratory like theirs. The second difference is that unlike Nishidome *et al.* (1994), the RBC disc was completely stopped in this study for DO measurement, as Nishidome and Kasuda (1988) did in their study. As a result, a comparison between our field results with their laboratory results would be meaningful.

In order to make such a comparison, above simplified assumption and the constant oxygen diffusivity which was used by above two groups has been accepted in this part of this thesis for estimations of oxygen flux into wastewater biofilms. A detailed calculation procedure is illustrated in Appendix 3.3. The calculated oxygen fluxes into wastewater biofilms at each RBC stage at both sites (Devon and Olds) are listed in Table 3.8.

As clearly shown in Table 3.8, oxygen flux at Devon ranges from 4.34 g/m²/day to 9.01 g/m²/day, while at Olds, it ranges from 7.23 g/m²/day to 11.03 g/m²/day. Due to the way oxygen flux was calculated, these are actually only average values for the whole depth of oxygen penetration in wastewater biofilms. If taking the first four stages as a whole in both RBC systems, then an average of 6.99 g/m²/day and 8.29 g/m²/day can be obtained for Devon and Olds, respectively.

In the study of Nishidome and Kasuda (1988), they reported an average oxygen flux into RBC biofilm at about 6 g/m²/day using an oxygen diffusion coefficient of 2.0×10^{-4} m²/day. While in the study of Nishidome *et al.* (1994), using an oxygen diffusion coefficient of 2.1×10^{-4} m²/day, an oxygen flux into RBC biofilms of 15 g/m²/day was reported.

Table 3.8 Oxygen flux into biofilms at each RBC stage at Devon and Olds

Unit: g/m ² /day			
Stage	Measurement spot	Devon	Olds
1	#1	5.65	11.03
	#2	4.34	7.94
2	#1	8.53	7.9
	#2	7.23	8.07
3	#1	5.29	8.64
	#2	-	7.23
	#3	-	7.77
	#4	-	7.91
4	#1	9.01	7.26
	#2	8.91	7.76
	#3	-	9.7
Average \pm SD*		6.99 \pm 1.91	8.29 \pm 1.13

* SD: Standard deviation.

Compared with the results of these published studies, the oxygen flux estimations in our field study seem to be much closer to Nishidome and Kasuda (1988), where the RBC was also stopped and had been exposed to the air phase for 60 seconds. This is reasonable because in both cases, wastewater biofilms had been exposed to the air phase for a period of time which was long enough for DO

penetration from the air into the biofilm to reach a steady state. The process for DO profiles in RBC biofilms to reach a steady status only takes several seconds after the RBC disc rotates out of the water phase to the air phase (Nishidome *et al.*, 1994).

While compared with Nishidome *et al.* (1994), oxygen flux of this field study does not agree very well. Theoretically, oxygen flux into biofilms on an alternately rotating RBC disc between the air and the water phases should be lower than that of a stopped RBC disc, because in the former case, there is an attached water formed over the biofilm, which impedes oxygen flux into the biofilm. This is also a problem when a comparison between Nishidome and Kasuda (1988) and Nishidome *et al.* (1994) is made. Possible reason may lie in factors associated with other experimental conditions rather than the factor of whether the RBC disc is stopped or not when the DO measurement is conducted in RBC biofilms.

As one of the important indexes in assessment of oxygen transfer in wastewater biofilms, the estimation of oxygen flux is an unavoidable issue in oxygen transfer study. However, it's still important to point out that wastewater biofilms are structurally heterogeneous. Various, instead of a constant, value(s) for oxygen diffusivities, once available, should be used in oxygen transfer study in biofilms, such as the estimation of oxygen flux into wastewater biofilms.

Chapter 4 Conclusions and Recommendations

This project has explored the feasibility of *in-situ* DO measurement in domestic wastewater biofilms directly under the field conditions with the adaptation of a newly developed combined oxygen microelectrode. Based upon the results from this study, the following conclusions and recommendations for future work are made.

4.1 Conclusions

- (1) All experimental results from this study have clearly shown that oxygen depletion existed within wastewater biofilms under field conditions. Only a shallow depth in wastewater biofilms was penetrated by oxygen. All measurements indicated that the depth of oxygen penetration was less than 600 μm . No full penetration of dissolved oxygen in the wastewater biofilms was observed. As a result, two layers within wastewater biofilms could be expected in terms of the existence of dissolved oxygen - an oxic layer on top and an anoxic layer underneath. This study has, for the first time, provided experimental evidence under field conditions to confirm the previous conclusion, drawn from laboratory observations, on oxygen depletion phenomenon in wastewater biofilms.
- (2) The phenomenon of partial oxygen penetration in the wastewater biofilms was observed at every stage of the four-stage RBC system and at both wastewater treatment plants, which are well-operated plants typical for domestic

wastewater treatment. Therefore, the results of this field study indicated that partial oxygen penetration could be a common phenomenon in wastewater biofilms in the field and the results themselves are more applicable to biofilm modeling and meaningful for the design and operation of domestic wastewater biofilm reactors.

- (3) The investigation into the differences in oxygen penetration depth in biofilms between these two wastewater treatment plants using similar RBC systems disclosed that oxygen penetration depth in biofilms with shorter length of operation was greater than that in biofilms with longer length of operation. If this relationship can be verified in future studies, there might be a significant meaning for the design and operation of wastewater biofilm reactors.
- (4) Compared with the possible influences from the type of substratum materials and the stage of RBC systems on oxygen penetration depth in wastewater biofilms, the influence from the location of dissolved oxygen measurement in wastewater biofilms was much more significant. In other words, the results from dissolved oxygen measurement in wastewater biofilms using oxygen microelectrode are site-specific. This was attributed to the heterogeneity of the structure and density of wastewater biofilms.
- (5) Oxygen flux is an important index for oxygen transfer study in biofilms. A number of laboratory studies have made estimations for this index by using a constant value for oxygen diffusivity in biofilms. Using the similar method but with the field data from our *in-situ* measurements, an estimation of oxygen flux into wastewater biofilms was made. As a result of this estimation, average

oxygen fluxes of 6.99 g/m²/day and 8.29 g/m²/day were obtained for wastewater biofilms in RBC systems at Devon and Olds, respectively. These results are in good agreement with similar RBC biofilm studies in laboratory. However, it is important to point out that wastewater biofilms are structurally heterogeneous. Various, instead of constant, value(s) for oxygen diffusivities, once available, should be used for oxygen transfer in biofilms such as the estimation of oxygen flux into wastewater biofilms.

- (6) The methodology used in this thesis was effective for the measurement of dissolved oxygen in wastewater biofilms under field conditions. The combined oxygen microelectrode was much less subject to external electromagnetic interference, compared with the separate oxygen microelectrode. The results of this thesis have also shown that the fabrication procedures developed in this study were effective.

4.2 Recommendations for future work

- (1) This study has accomplished an important step - to measure DO profile in wastewater biofilms under field conditions. This method has disclosed the nature of DO distribution in the vertical direction in wastewater biofilms. However, wastewater biofilms are heterogeneous both vertically and horizontally, which makes DO distributions in wastewater biofilms vary greatly. As a result, to obtain a more complete picture (i.e. 3-dimension profile) of DO distributions in wastewater biofilms would be a rational

direction for future study on the basis of this thesis work.

- (2) In order to fulfill above goal, and to improve the accuracy of similar studies, an automatic data acquisition system would be very helpful. In this system, the movement of the oxygen microelectrode and the signal recording can be synchronized and controlled in a computer installed with a controlling program. In this case, the resolution of the interval of depth and hence the quality of the DO profile can be improved greatly.
- (3) Adaptation of a combined optical density sensor and oxygen microelectrode can help more accurately determine the surface and the thickness of the biofilm.

References

- Baumgärtl, H., 1987. Systematic investigation of needle electrode properties in polarographic measurements of local tissue P_{O_2} . In *Clinical oxygen pressure measurement*. Ehrly, A.M., Hauss, J. and Huch, R(eds.) Springer-Verlag, New York. 17-42.
- Baumgärtl, H. and Lübbers, D.W., 1973. Platinum needle electrode for polarographic measurement of oxygen and hydrogen. In *Oxygen supply: theoretical and practical aspects of oxygen supply and microcirculation of tissue*. University Park Press, Baltimore, London, Tokyo. 130-137.
- Baumgärtl, H. and Lübbers, D.W., 1983. Microcoaxial needle sensor for polarographic measurement of local O_2 pressure in the cellular range of living tissue. Its construction and properties. In *Polarographic oxygen sensors: Aquatic and Physiological Applications*. (E. Gnaiger and H. Forstner, eds.), Springer-Verlag, New York, Heidelberg, 37-65.
- Bintanja H. H. J., van der Erve J.J.M. & Boelhouwer C., 1975 Oxygen transfer in a rotating disc treatment plant. *Water Research*, 9, 1147-1153.
- Bishop, P.L., 1997. Biofilm structure and kinetics. *Water Science and Technology*. 36(1), 287-294.
- Bishop, P. and Yu, T, 1999. A microelectrode study of redox potential change in biofilms. *Water Science and Technology*. 39 (7), 179-185.
- Bungay, H.R. 3rd and Chen, Y. S., 1981. Dissolved oxygen profiles in photosynthetic microbial slimes. *Biotechnology and Bioengineering*. 23, 1893-1895.
- Bungay, H.R. 3rd and Harold, Jr. D.M., 1971. Simulation of oxygen transfer in microbial slimes. *Biotechnology and Bioengineering*. 13, 569-579.
- Bungay, H.R. 3rd, Whalen, W.J. and Sanders, W.M., 1969. Microprobe techniques for determination diffusivities and respiration rates in microbial slime systems. *Biotechnology and Bioengineering*. 11, 765-772.

- Carter, D.B. and Silver, I.A., 1961. Microelectrodes and electrodes used in biology. In *Reference electrodes*. Ives, D.J.G. and Janz, J.G.(eds.) Academic Press, New York, 464-519.
- Chen, G. H., 1996. Prediction of oxygen limitation in an aerobic biofilm reactor. *Journal of Environmental Science and Health*, A31(10), 2465-2475.
- Chen, G. H. and Huang, J. C., 1996. Determination of diffusion layer thickness on a biofilm. *Journal of Environmental Science and Health*, A31(2), 367-386.
- Chen, Y.S. and Bungay, H.R., 1981. Microelectrode studies of oxygen transfer in trickling filter slimes. *Biotechnology and Bioengineering*. 23,781-792.
- Clark, Jr. L.C., Wolf, R., Granger, D. and Taylor, A., 1953. Continuous recording of blood oxygen tension by polarography. *Journal of Applied Physiology*. 6, 189-193.
- Davies, P.W. and Brink, F.Jr., 1942. Microelectrodes for measuring local oxygen tension in animal tissues. *Review of scientific instruments*. 13, 524-533.
- de Beer, D. and Schramm, A., 1999. Micro-environments and mass transfer phenomena in biofilms studied with microsensors. *Water Science and Technology*. 39(7), 173-178.
- Dowben, R.M. and Rose, J.E., 1953. A metal-filled microelectrode. *Science*, 118, 22 - 24.
- Ferris, C.D., 1974. *Introduction to Bioelectrodes*, Plenum Press, New York.
- Fu, Y.C., 1993. Characterizing oxygen profiles and determine oxygen diffusivity in biofilm during biodegradation of azo dyes. Ph.D. Dissertation, University of Cincinnati, Cincinnati, Ohio, USA.
- Fu, Y.C. and Bishop, P.L., 1993. The evaluation of respiration rate in fixed-film systems under various organic loading rates. In: *Proceedings of the Water Environment Federation 66th Annual Conference*. Water Environment Federation, 283-294.
- Fu, Y.C., Zhang, T.C. and Bishop, P.L., 1994. Determination of effective oxygen

diffusivity in biofilms grown in a completely mixed biodrum reactor. *Water Science and Technology*. 29 (10-11), 455-462.

Grady, C.P.L.Jr., Glen T.D. and Henry C.L., 1999. *Biological wastewater treatment*. 2nd edition, Marcel dekker, Inc., New York, USA.

Heineman, W.R. 1989. Voltammetry: basic concepts and hydrodynamic techniques. Chapter 29, in *Chemical instrumentation: A systematic approach*, 3rd edition, edited by H. A. Strobel and W. R. Heineman, John Wiley & Sons Inc., New York.

Hitchman, M.L. 1983. Calibration and accuracy of polarographic oxygen sensors. Chapter I.2, in *Polarographic oxygen Sensors, aquatic and physiological applications*, edited by E. Gnaiger and H. Forstner, Springer-Verlag, Berlin Heidelberg.

Horn, H. and Hempel, D.C., 1997. Substrate utilization and mass transfer in an autotrophic biofilm system: experimental results and numerical simulation. *Biotechnology and Bioengineering*. 53 (4), 363-371.

Horn, H. and Hempel, D.C., 1998. Modeling mass transfer and substrate utilization in the boundary layer of biofilm systems. *Water Science and Technology*. 37 (4-5), 139-147.

Kuenen, J.G., Jørgensen, B.B. and Revsbech, N.P., 1986. Oxygen microprofiles of trickling filter biofilms. *Water Research*. 20(12), 1589-1598.

Kugaprasatham, S., Nagaoka, H. and Ohgaki, S., 1992. Effect of Turbulence on nitrifying biofilms at non-limiting substrate conditions. *Water Research*, 26(12), 1692-1638.

Lewandowski, Z., Walser, G., Larsen, R., Peyton, B. and Characklis, W.G., 1990. Biofilm surface positioning. *Environmental Engineering Proceedings of the 1990 Specialty Conference*, Arlington, Virginia, July 8-11, 1990, ASCE. 17-24.

Lewandowski, Z., Walser, P. and Characklis, W.G., 1991. Reaction kinetics in biofilm. *Biotechnology and Bioengineering*. 38, 877-882.

- Lewandowski, Z., Altobelli, S.A. and Fukushima, E., 1993. NMR and microelectrode studies of hydrodynamics and kinetics in biofilms. *Biotechnology Progress*. 9(1), 40-45.
- Li, J. and Bishop, P.L., 2000. Microelectrode analysis of simultaneous nitrification/denitrification in biofilms. In *Proceedings of ASM Conference on Biofilms 2000 (B2K)*, July 16-20, 2000, Big Sky, Montana, USA.
- Linsenmeier, R.A. and Yancy, C.M., 1987. Improved fabrication of double-barreled recessed cathode O₂ microelectrodes. *The American Physiological Society*, 63 (6), 2254-2557.
- Nielsen, L.P., Christensen, P.B., Revsbech, N.P. and Sorensen, J., 1990. Denitrification and oxygen respiration in biofilms studied with a microsensor for nitrous oxide and oxygen. *Microbial Ecology*. 19, 63-72.
- Nishidome K. and Kusuda, T., 1988. Measurements of dissolved oxygen in attached microbial films of rotating biological contactor by oxygen microelectrode. In *Proceeding of Second IAWPC Asian conference on water pollution (Advanced Water Pollution Control No.6)*, 305-311.
- Nishidome K., Kusuda, T., Watanabe, Y., Yamauchi, M. and Mihara, M., 1994. Determination of oxygen transfer rate to a rotating biological contactor by microelectrode measurement. *Water Science and Technology*. 29(10-11), 471-477.
- Rasmussen, K. and Lewandowski, Z., 1998a. Microelectrode measurements of local mass transfer rates in heterogeneous biofilms, *Biotechnology and Bioengineering*. 59(3), 302-309.
- Rasmussen, K. and Lewandowski, Z., 1998b. The accuracy of oxygen flux measurements using microelectrodes. *Water Research*. 32(12), 3747-3755.
- Revsbech, N.P., 1983. *In situ* measurement of oxygen profiles of sediments by use of oxygen microelectrodes. In *Polarographic oxygen sensors: Aquatic and Physiological Applications*. E. Gnaiger and H. Forstner, eds., Springer-Verlag, New York, Heidelberg, 265-273.
- Revsbech, N.P., 1989. An oxygen microsensor with a guard cathode. *Limnology and*

Oceanography. 34(2), 474-478.

Revsbech, N.P. and Jørgensen, B.B., 1986. Microelectrodes: their use in microbial ecology. In *Advances in Microbial Ecology*. 9, 293-352.

Revsbech, N.P., and Ward, D.M., 1983. Oxygen microelectrode that is insensitive to medium chemical composition: use in an acid microbial Mat dominated by *Cyanidium caldarium*, *Applied and Environmental Microbiology*. 45(3), 755-759.

Revsbech, N.P., Jørgensen, B.B. and Blackburn, T.H., 1980. Oxygen in the sea bottom measured with a microelectrode. *Science*. 207,1355-1356.

Revsbech, N.P., Jørgensen, B.B. and Blackburn, T.H., 1983. Microelectrode studies of the photosynthesis and O₂, H₂S, and pH profile of a microbial Mat. *Limnology and Oceanography*. 28(6),1062-1074.

Sanders W.M., Bungay H.R. and Whalen W.J., 1971. Oxygen microprobe studies of microbial slime films. In *Water-1970*, L.K. Cecil, Ed., *American Institute of Chemical Engineers Symposium*, 107, 69-74.

Santegoeds, C.M., Muyzer, G. and DeBeer, D., 1998. Biofilm dynamics studied with microsensors and molecular techniques. *Water Science and Technology*. 37 (4-5), 125-129.

Spengel, D.B., D.A. Dzombak, 1992. Biokinetic modeling and scale-up considerations for rotating biological contactors. *Water Environment Research*, 64(3), 223-235.

Ward, D.M., Bateson, M.M., Weller, R. and Ruff-Roberts, A.L., 1992. Ribosomal RNA analysis of micro-organisms as they occur in nature. In *Advances in Microbial Ecology*. 12, 219-286.

Watanabe, Y., Ishiguro M. and Nishidome, K., 1980. Nitrification kinetics in a rotating biological disc reactor. *Water Science and Technology*. 12(6), 233-251.

Watanabe, Y., Bravo, M. and Nishidome, K., 1982. Simulation of nitrification and its dynamics in a rotating biological contactor. *Water Science and Technology*. 14(8), 811-832.

- Whalen, W.J., Riley, J. and Nair, P., 1967. A microelectrode for measuring intracellular P_{O_2} . *Journal of Applied Physiology*, 23, 798-801.
- Whalen, W.J., Bungay, H.R. III and Sanders, W.M. III, 1969. Microelectrode determination of Oxygen profiles in microbial slime systems. *Environmental Science and technology*. 3(12), 1297.
- Williamson, K. and McCarty, P.L., 1976. A model of substrate utilization by bacterial films. *Journal of Water Pollution Control Federation*, 8(1), 9-24.
- Yellow Spring Instruments Incorporated. *YSI MODEL 50B Dissolved Oxygen Meter Instructions*. Yellow Springs, Ohio, USA.
- Yu, T., 2000. Stratification of microbial processes and redox potential changes in biofilms. PhD Dissertation, University of Cincinnati, Cincinnati, Ohio, USA.
- Yu, T. and Bishop, P.L., 1998. Stratification of microbial metabolic processes and redox potential change in an aerobic biofilm studied using microelectrodes. *Water Science and Technology*. 37 (4-5), 195-198.
- Zeevalkink, J.A., Kelderman P. And Boelhouwer C., 1978. Liquid film thickness in a rotating disc gas-liquid contactor. *Water Research*, 12, 577-581.
- Zhang, T.C., 1994. Influence of biofilm structure on transfer and transformation processes in biofilm. PhD Dissertation, University of Cincinnati, Cincinnati, Ohio, USA.
- Zhang, T.C. and Bishop, P.L., 1994a. Density, porosity and pore structure of biofilms. *Water Research*, 28, 2267-2277.
- Zhang, T.C. and Bishop, P.L., 1994b. Evaluation of substrate and pH effects in a nitrifying biofilm. In: *Proceedings of the Water Environment Federation 67th Annual Conference*. Water Environment Federation, 519-530.
- Zhang, T.C. and Bishop, P.L., 1994c. Experimental determination of the dissolved oxygen boundary layer and mass transfer resistance near the fluid-biofilm interface. *Water Science and Technology*. 30(11), 47-58.

Zhang, T., Fu, Y. and Bishop, P., 1994. Competition in biofilms. *Water Science and Technology*. 29(10-11), 263-270.

Zhang, T., Fu, Y. and Bishop, P., 1995. Competition for substrate and space in biofilms. *Water Environment Research*. 67, 992-1003.

Appendices

Appendix 2.1

Table A2-1: Calibration process data for Figure 2.4 *

Time(seconds)	Condition	Reading (pA)	Time(seconds)	Condition	Reading (pA)
0	N ₂ -flushing	598	900		11
20		214	920		9
40		119	940		7
60		71	960		6
80		44	980		6
100		28	1000	stop N ₂ -flushing	6
120		18	1020		6
140		13	1040		6
160		9	1060	switch to air-flushing	6
180		8	1080		452
200		7	1100		531
220		6	1120		571
240		6	1140		596
260		6	1160		606
280		6	1180		619
300	Stop N ₂ .flushing	6	1200		623
320		6	1220		625
340		6	1240		624
360		6	1260	stop air-flushing	625
380	switch to air-flushing	6	1280		599
400		473	1300		598
420		524	1320		597
440		574	1340		598
460		598	1360	re-air-flushing	599
480		615	1380		625
500		620	1400		624
520		624	1420		625
540		625	1440		625
560	stop air-flushing	624	1460	switch to N ₂ -flushing	624
580		599	1480		215
600		598	1500		120
620		599	1520		68
640		598	1540		44
660	re-air-flushing	599	1560		27
680		626	1580		18
700		625	1600		13
720		624	1620		10
740		625	1640		9
760	switch to N ₂ -flushing	625	1660		7
780		198	1680		6
800		97	1700	stop N ₂ -flushing	6
820		54	1720		6
840		31	1740		6
860		23	1760		6
880		14		switch to 10.5% O ₂ -flushing	

*Water temperature: 20°C

Appendix 2.2

Table A2-2: Data of the three-point calibration process for Figure 2.5

Condition*	Reading (pA)	Average (pA)
Oxygen-free	6, 6, 6, 6, 6	6
10.5% O ₂	303, 302, 303, 304, 303	303
Air-saturated	598, 599, 599, 598, 599	599

*: Stagnant water and its temperature at 20°C.

Appendix 3.1

Data for Figure 3.4 (data from Stage 4 - spot 2 at Olds)

Oxygen microelectrode	Depth	Current signal
Position	(μm)	(pA)
0	-500	731
1	-450	730
2	-400	726
3	-350	729
4	-300	729
5	-250	726
6	-200	735
7	-150	721
8	-100	718
9	-50	726
10	0	725
11	50	493
12	100	319
13	150	252
14	200	165
15	250	100
16	300	63
17	350	43
18	400	23
19	450	16
20	500	7
21	550	6
22	600	6

Appendix 3.2

Data for constructions of DO profiles from Figure 3.5 to Figure 3.12

In-situ DO data at Olds - for Figure 3.5 to Figure 3.8.

Stage 1				Stage 3							
Spot 1 (P1)		Spot 2 (P2)		Spot 1 (P1)		Spot 2 (P2)		Spot 3 (P3)		Spot 4 (P4)	
Depth (µm)	DO (mg/L)	Depth (µm)	DO (mg/L)	Depth (µm)	DO (mg/L)	Depth (µm)	DO (mg/L)	Depth (µm)	DO (mg/L)	Depth (µm)	DO (mg/L)
0	11.67	0	10.92	0	11.90	0	11.40	0	10.63	0	10.66
50	4.80	50	6.63	50	7.59	50	10.31	50	6.76	50	7.02
100	3.59	100	4.89	100	5.96	100	6.63	100	5.40	100	5.22
150	1.95	150	3.01	150	3.58	150	5.80	150	4.50	150	4.22
200	1.27	200	1.75	200	2.86	200	3.16	200	3.27	200	3.27
250	0.83	250	1.24	250	2.01	250	1.52	250	2.10	250	1.54
300	0.76	300	1.00	300	1.32	300	0.37	300	1.28	300	0.82
350	0.41	350	0.88	350	0.73	350	0.23	350	0.90	350	0.23
400	0.14	400	0.69	400	0.65	400	0.12	400	0.44	400	0.18
450	0.03	450	0.39	450	0.08	450	0.00	450	0.15	450	0.13
500	0.00	500	0.18	500	0.05	500	0.00	500	0.00	500	0.00
550	0.00	550	0.06	550	0.00	550	0.00	550	0.00	550	0.00
600	0.00	600	0.00	600	0.00			600	0.00	600	0.00
		650	0.00	650	0.00						
		700	0.00								

Stage 2				Stage 4					
Spot 1 (P1)		Spot 2 (P2)		Spot 1 (P1)		Spot 2 (P2)		Spot 3 (P3)	
Depth (µm)	DO (mg/L)	Depth (µm)	DO (mg/L)	Depth (µm)	DO (mg/L)	Depth (µm)	DO (mg/L)	Depth (µm)	DO (mg/L)
0	11.48	0	10.59	0	10.15	0	10.13	0	10.35
50	6.46	50	7.11	50	5.75	50	6.85	50	6.09
100	5.50	100	5.71	100	4.41	100	4.38	100	4.22
150	4.61	150	4.19	150	3.63	150	3.43	150	2.71
200	3.60	200	3.20	200	3.20	200	2.20	200	1.37
250	2.68	250	1.51	250	2.13	250	1.28	250	0.58
300	2.31	300	0.86	300	1.05	300	0.75	300	0.35
350	1.75	350	0.33	350	0.57	350	0.47	350	0.11
400	1.40	400	0.06	400	0.33	400	0.18	400	0.00
450	0.24	450	0.00	450	0.24	450	0.09	450	0.00
500	0.22	500	0.00	500	0.20	500	0.00	500	0.00
550	0.06	550	0.00	550	0.09	550	0.00		
600	0.00			600	0.00	600	0.00		
650	0.00			650	0.00				
700	0.00			700	0.00				

***In-situ* DO data at Devon - for Figure 3.9 to Figure 3.12.**

Stage 1													
Spot 1 (P1)		Spot 2 (P2)		Spot 3 (M1)		Spot 4 (M2)		Stage 3		Stage 4			
Spot 1 (P1)		Spot 2 (P2)		Spot 3 (M1)		Spot 4 (M2)		Spot 1 (P1)		Spot 1 (P1)		Spot 2 (P2)	
Depth (µm)	DO (mg/L)	Depth (µm)	DO (mg/L)	Depth (µm)	DO (mg/L)	Depth (µm)	DO (mg/L)	Depth (µm)	DO (mg/L)	Depth (µm)	DO (mg/L)	Depth (µm)	DO (mg/L)
0	8.31	0	8.46	0	9.10	0	8.54	0	9.28	0	9.60	0	9.93
50	7.76	50	7.84	30	6.39	50	7.69	50	7.51	50	6.97	50	7.26
80	6.50	100	7.13	60	4.93	80	7.13	100	6.82	80	4.66	80	4.87
110	4.94	150	5.02	90	3.61	110	6.21	150	4.58	110	3.81	110	3.79
140	3.84	200	4.00	120	2.22	140	5.58	200	3.61	140	2.40	140	2.81
170	3.06	250	2.35	150	1.39	170	4.45	250	2.46	170	1.65	170	1.78
200	2.19	300	0.94	180	0.49	200	3.03	300	1.32	200	1.04	200	1.41
230	1.18	350	0.24	210	0.07	230	2.40	350	0.46	230	0.71	230	0.75
260	0.47	400	0.00	240	0.00	260	1.41	400	0.23	260	0.38	260	0.33
290	0.16	450	0.00	270	0.00	290	0.92	450	0.11	290	0.19	290	0.23
320	0.08	500	0.00	300	0.00	320	0.71	500	0.06	320	0.09	320	0.09
350	0.00					350	0.49	550	0.00	350	0.00	350	0.05
380	0.00					380	0.35	600	0.00	380	0.00	380	0.00
410	0.00					410	0.28	650	0.00	410	0.00	410	0.00
						440	0.14	700	0.00			440	0.00
						470	0.07	750	0.00				
						500	0.00	tip broken					
						530	0.00	at this depth					
						560	0.00						

Stage 2											
Spot 1 (P1)		Spot 2 (P2)		Spot 3 (M1)		Spot 4 (M2)		Spot 5 (M3)		Spot 6 (M4)	
Depth (µm)	DO (mg/L)	Depth (µm)	DO (mg/L)	Depth (µm)	DO (mg/L)	Depth (µm)	DO (mg/L)	Depth (µm)	DO (mg/L)	Depth (µm)	DO (mg/L)
0	9.44	0	9.42	0	9.23	0	8.98	0	8.58	0	8.67
30	7.45	30	7.91	50	7.70	30	8.49	30	5.85	30	7.52
60	5.88	60	6.31	100	6.73	60	6.34	60	4.56	60	5.92
90	4.99	90	5.91	150	4.99	90	5.49	90	3.39	90	4.02
120	4.06	120	4.93	200	3.51	120	4.91	120	1.88	120	2.70
150	3.05	150	4.13	250	2.20	150	3.71	150	0.98	150	1.44
180	2.71	180	3.64	300	1.02	180	2.90	180	0.54	180	0.63
210	1.82	210	2.49	350	0.34	210	2.19	210	0.22	210	0.11
240	1.27	240	1.55	400	0.04	240	1.74	240	0.00	240	0.00
270	0.68	270	1.16	450	0.00	270	1.16	270	0.00	270	0.00
300	0.34	300	0.84	500	0.00	300	0.80	300	0.00	300	0.00
330	0.08	330	0.58	550	0.00	330	0.45				
360	0.00	360	0.13			360	0.13				
390	0.00	390	0.00			390	0.00				
420	0.00	420	0.00			420	0.00				
		450	0.00			450	0.00				

Appendix 3.3

An example for estimation of oxygen flux in wastewater biofilms

Oxygen flux into wastewater biofilm is estimated from the following equation:

$$F = D_b \cdot (C_0 - C_d) / d \quad (A-1)$$

Where,

F = Oxygen flux into biofilm ($\text{g/m}^2/\text{day}$);

D_b = Oxygen diffusion coefficient in biofilm (literature value, $2.1 \text{cm}^2/\text{day}$);

C_0 = DO concentration at biofilm surface (g/m^3);

C_d = DO concentration at depth (d) in biofilm (g/m^3);

d = Depth in biofilm from the biofilm surface (m).

The data for the following calculation are from DO profile of Stage 4-spot2 at Olds.

Depth (m)	DO (g/m^3)	Oxygen flux ($\text{g/m}^2/\text{d}$)
0	10.13	13.81
0.00005	6.85	12.08
0.0001	4.38	9.38
0.00015	3.43	8.33
0.0002	2.20	7.44
0.00025	1.28	6.57
0.0003	0.75	5.80
0.00035	0.47	5.22
0.0004	0.18	4.69
0.00045	0.09	4.26
0.0005	0.00	Average = 7.76

As a result, the average oxygen flux into the biofilm at this spot is $7.76 \text{ g/m}^2/\text{d}$.

University of Alberta Library



0 1620 1423 4122

B45617